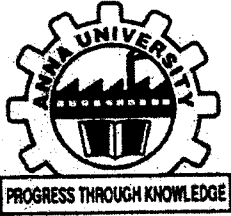


P-1411



FACTS- BASED POWER FLOW CONTROL IN INTER-CONNECTED POWER SYSTEMS

by

N. Geetha Rani
 Reg. No 71203415005



of

**KUMARAGURU COLLEGE OF TECHNOLOGY
 COIMBATORE**

**A PROJECT REPORT
 Submitted to the**

**FACULTY OF ELECTRICAL & ELECTRONICS
 ENGINEERING**

*In partial fulfillment of the requirements
 for the award of the degree*

of

MASTER OF ENGINEERING

IN

POWER ELECTRONICS & DRIVES

JUNE 2005

BONAFIDE CERTIFICATE

Certified that this project report titled **FACTS- BASED POWER FLOW CONTROL IN INTER-CONNECTED POWER SYSTEMS** is the bonafide work of Ms. N.GEETHARANI who carried out the research under my supervision. Certified further, that to the best of my knowledge the work reported herein does not form part of any other project report or dissertation on the basis of which a degree or award was conferred on an earlier occasion on this or any other candidate.


04/6/05
PROJECT GUIDE


HEAD OF THE DEPARTMENT

The Candidate with University Register No: 71203415005 was examined by us in the project Viva-Voce examination held on 23-6-2005


INTERNAL EXAMINER


EXTERNAL EXAMINER

ABSTRACT

The control of power flow along the transmission line to meet the needs of power transfer has become more and more important. The fast development of power electronics technology has made FACTS a promising pattern of future power system. With this FACTS technology such as STATCOM, TCSC, TCPR, UPFC etc. the bus voltage, line impedance, phase angles in the power system can be regulated rapidly and flexibly.

FACTS facilitate the power flow control, enhance the power transfer capability, decrease generation cost and improve the security and stability of power system. However in the inter-connected power systems installed with one or more FACTS devices is necessary to analyze the power flow controllability especially to determine the control range of transmission line installed with FACTS devices and to coordinate the control performance of several FACTS devices in power system

In this paper based on the steady state model of FACTS devices, the controllability and control range of power flow on transmission line installed with various types of FACTS devices are analytically investigated first. By the use of load flow steady program with the consideration of these FACTS devices power flow control ranges are drawn.

Genetic algorithm can deal with non-smooth discontinuous and non-differentiable function which may be confronted in power flow control with FACTS devices and search for the global optimum in a complicated and uncertain region, a new genetic algorithm based optimization method is developed to analyze the coordination of power flow control in power system installed with several FACTS devices. With this proposed method the maximal, power flow control range in any or any set of transmission line can be obtained.

ACKNOWLEDGEMENT

First and foremost, I would like to extend my heart-felt gratitude and thanks to our beloved Principal of Kumaraguru College of Technology, **Dr.K.K.PADMANABHAN** without whom I would not have been studying in this institution.

I wish to thank our H.O.D **Prof. REGUPATHY SUBRAMANIAM** for offering his generous support during the course of this work.

I express my profound sense of gratitude to **Mrs. R.MAHALAKSHMI** for her systematic guidance, valuable advice and constant encouragement throughout this project work.

I am also indebted to **Dr. T.M.KAMESWARAN**, our Advisor **Mrs. N.KALAIARASI M.E.**, for the helping hand they extended during trying periods while doing the project. I am very much grateful to all other staff members of Electrical & Electronics Engineering Department who extended all kind of cooperation for the completion of this work.

The constant guide and care showered upon me by my **PARENTS** is untold and immeasurable. Finally, it give me a great pleasure to express my sincere thanks to all my **FRIENDS** who have helped me during the course of this work.

TABLE OF CONTENTS

Chapter	Title	Page No
	ABSTRACT	iii
	LIST OF FIGURES	viii
1.	INTRODUCTION	1
	1.1 INTRODUCTION OF FACTS DEVICES	1
	1.2 AIM OF THE PROJECT	2
	1.3 WHY WE NEED TRANSMISSION INTERCONNECTIONS	2
	1.4 IMPACT OF FACTS IN INTERCONNECTED NETWORKS	2
	1.5 INTRODUCTION TO FACTS CONTROLLERS	3
	1.5.1 Definition of FACTS	3
	1.5.2 FACTS categories and their functions	4
	1.5.3 Typical FACTS devices and their function	5
2.	FACTS DEVICES UNDER STUDY	7
	2.1 THYRISTOR-CONTROLLED SERIES CAPACITOR (TCSC)	7
	2.2 THYRISTOR CONTROLLED PHASE ANGLE REGULATOR	10
	2.3 UNIFIED POWER FLOW CONTROL	12
3.	COORDINATION OF POWERFLOW CONTROL - FACTS DEVICES	18
	3.1 BASIC PRINCIPLES OF POWER FLOW CONTROL WITH FACTS DEVICES	18
	3.1.1 Steady-State Models of FACTS Devices	18
	3.1.2 Power Flow Control Range with FACTS Devices	18
	3.2 14 BUS SYSTEM	20
	3.3 UNIFIED POWER FLOW CONTROLLER	21
	3.4 THYRISTOR-CONTROLLED SERIES COMPENSATOR	24
	3.5 THYRISTOR-CONTROLLED PHASE ANGLE REGULATOR	26
	3.6 POWER FLOW CONTROL RANGES	28

4	GENETIC ALGORITHM	29
	4.1 INTRODUCTION TO GENETIC ALGORITHM	29
	4.2 SOLUTION MODELING	30
	4.3 COORDINATION OF POWER FLOW CONTROL BASED ON GA	31
	4.4 MODELLING OF POWER FLOW CONTROL WITH FACTS DEVICES	32
	4.5 IMPROVED GENETIC ALGORITHM	33
	4.5.1 Objective Function	33
	4.5.2 Encoding	34
	4.5.3 Initial population	35
	4.5.4 Statistics	35
	4.5.5 Fitness calculation	36
	4.5.6 Reproduction	37
	4.5.7 Crossover	38
	4.5.8 Mutation	40
	4.5.9 Flow chart of the GA optimization	41
5.	SIMULATED OUTPUT RESULTS.	42
	5.1 TCSC OUTPUT RESULT	42
	5.2 TCPAR OUTPUT RESULTS	44
	5.3 UPFC OUTPUT RESULT	45
6.	HARDWARE IMPLEMENTATION	47
	6.1 INTRODUCTION TO HARDWARE IMPLEMENTATION	47
	6.2 CIRCUIT DIAGRAM	48
	6.3 CIRCUIT DESCRIPTION	49
	6.3.1 Aim of this implementation	49
	6.3.2 TCPAR Prototype Circuit and Hardware Design	49
	6.3.3 Power Supply Unit	49
	6.3.4 LM 741 comparator	50
	6.3.5 Reset inverter	51
	6.3.6 ATMEL 89C2051	51

6.3.7 Pin description	52
6.3.8 MOC3052-M optoisolators triac drivers	53
6.3.9 Output unit	54
7. CONCLUSION	55
APPENDIX 1 – UPFC Codings	
APPENDIX 2 – TCSC Codings	
APPENDIX 3- TCPAR Codings	
APPENDIX 4- Genetic algorithm implementation	
APPENDIX 5-UPFC Datas	
APPENDIX 6-TCSC Datas	
APPENDIX 7-TCPAR Datas	
APPENDIX 8-Microcontroller Codings	
REFERENCES	

LIST OF FIGURES

	Title	Page No
Figure 1.1.	TCSC	5
Figure 1.2.	TCPAR	5
Figure 1.3.	UPFC	6
Figure 2.1.	Thyristor-Controlled Series Capacitor (TCSC)	7
Figure 2.2.	Waveforms at various boost factors in capacitive boost mode	9
Figure 2.3.	Waveforms at various boost factors in inductive boost mode	10
Figure 2.4.	TCPAR	10
Figure 2.5.	Transmitted power versus angle characteristics for a Phase Angle Regulator	11
Figure 2.6.	$\partial P/\partial \sigma$ versus p	12
Figure 2.7.	Phasor diagrams illustrating the operation of the Unified power flow controller	15
Figure 2.8.	Implementation of the unified power-flow controller using two voltage-sourced inverters with a direct voltage link	17
Figure 3.1.	The unified model of FACTS devices in steady state	19
Figure 3.2.	Model of the transmission line installed with a FACTS device	19
Figure 3.3.	14 bus system	20
Figure 3.4.	Model of a TCSC	25
Figure 3.5.	Model of TCPAR	26
Figure 3.6.	S_{ij} close to the origin	28
Figure 3.7.	S_{ij} far away from origin	28
Figure 4.1.	String structure for the coordination of power flow controllers	33
Figure 4.2.	Individual configuration of FACTS devices	34
Figure 4.3.	Calculation of the entire population	36
Figure 4.4.	Roulette wheel selection	38
Figure 4.5.	Individuals	39

Figure 4.6. Offspring before correction	39
Figure 4.7. Offspring after correction	39
Figure 4.8. Flowchart	41
Figure 5.1. TCSC before optimization	42
Figure 5.2. Error minimization	43
Figure 5.3. TCSC after optimization	44
Figure 5.4. TCPR before optimization	44
Figure 5.5. TCPR after optimization	45
Figure 5.6. Before optimization	45
Figure 5.7. UPFC after optimization	46
Figure 6.1. Basic thyristor tap changer circuit configuration	47
Figure 6.2. Circuit Diagram	48
Figure 6.3. Power supply unit	50
Figure 6.4. Comparator	51
Figure 6.5. Pin diagram	52
Figure 6.6. Optoisolator and TRIAC drivers	53
Figure 6.7. Output waveform	54

CHAPTER 1

INTRODUCTION

1.1 INTRODUCTION OF FACTS DEVICES

With the rapid development of power electronics, Flexible AC Transmission Systems (FACTS) devices have been proposed and implemented in power systems. FACTS Devices can be utilized to control power flow and enhance system stability. Particularly With the deregulation of the electricity market, there is an increasing interest in using FACTS devices in the operation and control of power systems with new loading and Power flow conditions. A better utilization of the existing power systems to increase their capacities and controllability by installing FACTS devices becomes imperative. Due to the present situation, there are two main aspects that should be considered in using FACTS device

The first aspect is the flexible power system operation according to the power flow control capability of FACTS devices. The other aspect is the improvement of transient and steady-state stability of power systems.

FACTS devices are the right equipment to meet these challenges. Fast development and further extension of power systems can therefore be expected mainly in the areas of developing and emerging countries. However, because of a lack on available investments, the development of transmission systems in these countries does not follow the increase in power demand. Hence, there is a gap between transmission capacity and actual power demand, which leads to technical problems in the overloaded transmission systems. Interconnection of separated grids in the developed countries can solve some of these problems, however, when the interconnections are heavily loaded due to an increasing power exchange, the reliability and availability of the transmission will be reduced.

1.2 AIM OF THE PROJECT

The controllability and control range of power flow on transmission line installed with various types of FACTS devices are analytically investigated. there are several such devices in the system, coordination of power flow control performances of these devices can be defined as an optimization problem. By use of the load flow study program with the consideration of these FACTS devices power flow control ranges for these devices in a 5-bus system and in the IEEE 14-bus system arc drawn. . To solve this problem, an improved genetic algorithm based method has been developed. With this method, the power flow control ranges on one or a set of transmission lines in the power system installed with FACTS devices can be precisely computed and the maximal power flow control range on any or any set of transmission lines can be obtained.

1.3 WHY WE NEED TRANSMISSION INTERCONNECTIONS

We need these interconnections because apart from delivery, the purpose of the transmission network is to pool power plants and load centers in order to minimize the total power generation capacity and fuel cost. Transmission interconnections enables taking advantage of diversity of loads, availability of sources and fuel price in order to supply electricity to the loads at minimum cost with a required reliability. Inter connection is done for economic reasons, to reduce the cost of electricity and to improve reliability of power supply.

1.4 IMPACT OF FACTS IN INTERCONNECTED NETWORKS

The benefits of power system interconnection are well established. It enables the participating parties to share the benefits of large power systems, such as optimization of power generation, utilization of differences in load profiles and pooling of reserve capacity.

From this follows not only technical and economical benefits, but also environmental, when for example surplus of clean hydro resources from one region can help to replace polluting fossil-fuelled generation in another. For interconnections to serve their purpose, however, available transmission links must be powerful enough to safely transmit the amounts of power intended. If this is not the case, from a purely technical point of view it can always be remedied by building additional lines in parallel with the existing, or by updating the existing system to a higher voltage.

This, however, is expensive, time-consuming, and calls for elaborate procedures for gaining the necessary permits. Also, in many cases, environmental considerations, popular opinion or other impediments will render the building of new lines as well as updating to ultrahigh system voltages impossible in practice. This is where FACTS comes in. Examples of successful implementation of FACTS for power system interconnection can be found among others between the Nordic Countries (Nodal), and between Canada and the United States. In such cases, FACTS helps to enable mutually beneficial trade of electric energy between the countries. Other regions in the world where FACTS is emerging as a means for AC bulk power interchange between regions can be found in South Asia as well as in Africa and Latin America.

1.5 INTRODUCTION TO FACTS CONTROLLERS

1.5.1 Definition of FACTS

According to IEEE, FACTS, which is the abbreviation of Flexible AC Transmission Systems, is defined as follows, Alternating current transmission systems incorporating power electronics based and other static controllers to enhance controllability and power transfer capability. Since the "other static controllers" based FACTS devices are not widely used in Current power systems, this thesis focuses only on the power electronics based FACTS Devices.

1.5.2 FACTS categories and their functions

FACTS categories

In general, FACTS devices can be divided into four categories

Series FACTS devices:

Series FACTS devices could be a variable impedance, such as capacitor, reactor, etc. Or a power electronics based variable source of main frequency, sub synchronous and Harmonic frequencies (or a combination) to serve the desired need. In principle, all Series FACTS devices inject voltage in series with the transmission line.

Shunt FACTS devices:

Shunt FACTS devices may be variable impedance, variable source, or a combination of these. They inject current into the system at the point of connection.

Combined series-series FACTS device:

Combined series-series FACTS device is a combination of separate series FACTS Devices, which are controlled in a coordinated manner

Combined series-shunt FACTS device:

Combined series-shunt FACTS device is a combination of separate shunt and series Devices, which are controlled in a coordinated manner or one device with series and Shunt elements.

1.5.3 Typical FACTS devices and their functions

In this project, three typical FACTS devices are considered in detail: TCSC (Thyristor Controlled Series Capacitor), TCPST (Thyristor Controlled Phase Shifting Transformer), UPFC (Unified Power Flow Controller)

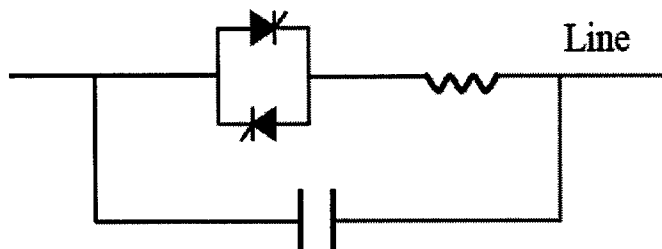


Figure 1.1 TCSC

TCSC is a typical series FACTS device that is used to vary the reactance of the Transmission line. Since TCSC works through the transmission system directly, it is Much more effective than the shunt FACTS devices in the application of power flow Control and power system oscillation damping control.

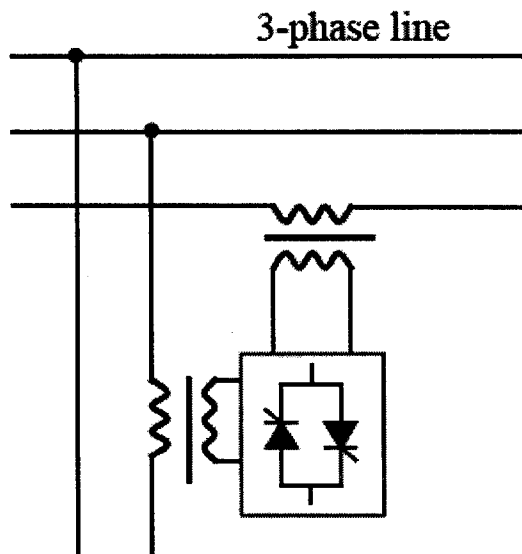


Figure 1.2 TCPAR

TCPAR is also a typical combined series-shunt FACTS device which can be used to regulate the phase angle difference between the two terminal voltages.

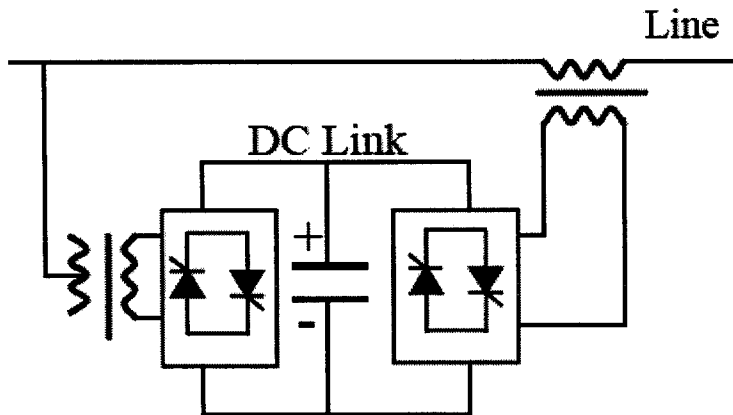


Figure1.3 UPFC

The UPFC is the most powerful and versatile FACTS device due to the facts that the Line impedance, terminal voltages, and the voltage angles can be controlled.

CHAPTER 2

FACTS DEVICES UNDER STUDY

2.1 THYRISTOR-CONTROLLED SERIES CAPACITOR (TCSC)

TCSC: A capacitive reactance compensator which consists of a series capacitor bank shunted by a thyristor-controlled reactor in order to provide a smoothly variable series capacitive reactance.

The scheme of a Thyristor-Controlled Series Capacitor is given in Fig. A Para-meter to describe the TCSC main circuit is λ which is the quotient of the resonant frequency and the network frequency resulting in

$$\lambda = \sqrt{\frac{-X_c}{X_L}} \quad (2.1)$$

Where $X_c = -1/\omega c$ and $X_L = \omega L$

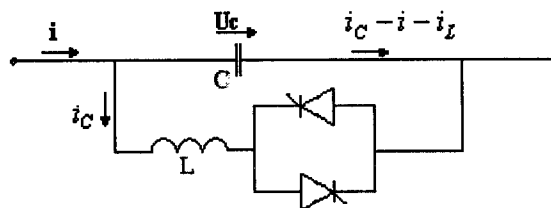


Figure 2.1. Thyristor-Controlled Series Capacitor (TCSC)

The operating modes of a TCSC are characterized by the so-called boost factor

$$K_B = X_{TCSC} / X_C \quad (2.2)$$

Where X_{TCSC} is the apparent reactance

1. **Blocking mode:** The thyristor valve is not triggered and the thyristors are kept in no conducting state. The line current passes only through the capacitor Bank ($X_{TCSC} = X_C$). Thus, the boost factor is equal to one. In this mode the TCSC performs like a fixed series capacitor.

2. **Bypass mode:** The thyristor valve is triggered continuously and therefore the Valve stays conducting all the time. The TCSC behaves like a parallel connection Of the series capacitor and the inductor.

$$X_{TCSC} = \frac{X_L X_C}{X_L + X_C} = \frac{-X_C}{1 - \lambda^2} \quad (2.3)$$

The voltage is inductive and the boost factor is negative. When X_L is considerably larger than unity the amplitude of X_C is much lower in bypass than in blocking mode. Therefore, the bypass mode is utilized to reduce the capacitor stress during faults.

3. **Capacitive boost mode:** If a trigger pulse is supplied to the thyristor having forward voltage just before the capacitor voltage crosses the zero line a capacitor discharge current pulse will circulate through the parallel inductive branch. The discharge current pulse adds to the line current through the capacitor bank. It Causes a capacitor voltage that adds to the voltage caused by the line current. The capacitor peak voltage thus will be increased in proportion to the charge that passes through the thyristor branch. The charge depends on the conduction angle β Figure 2.2 for the boost factor, the mathematical formula is (without giving the derivation)

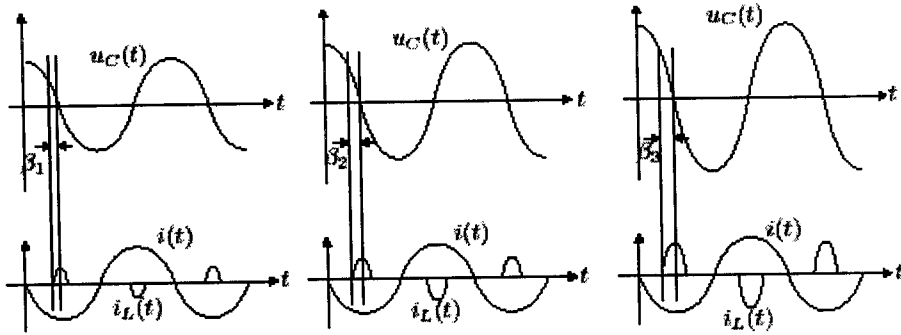


Figure 2.2. Waveforms at various boost factors in capacitive boost mode

$$K_B = 1 + \frac{2}{\pi} \frac{\lambda^2}{\lambda^2 - 1} \left[\frac{2 \cos^2 \beta}{\lambda^2 - 1} (\lambda \tan \lambda \beta - \tan \beta) - \beta - \frac{\sin 2\beta}{\beta} \right] \quad (2.4)$$

Due to the factor $\tan(\lambda\beta)$ this formula has an asymptote at β_∞ . The TCSC operates in the capacitive boost mode when $0 < \beta < \beta_\infty$

4. Inductive boost mode: If the conduction angle is increased above the mode changes from conductive to inductive boost mode Fig. In the inductive boost mode, large thyristor currents may occur. The curves of the currents and the voltage for three different conduction angles are given in Figure 2.3. The capacitor voltage waveform is very much distorted from its desired sinusoidal shape. Because of this waveform and the high valve stress, the inductive boost mode is less attractive for steady state operation.

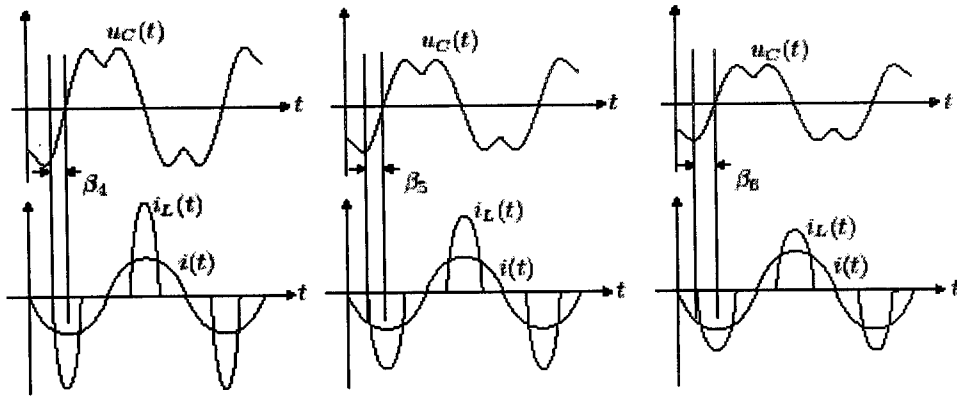


Figure 2.3 Waveforms at various boost factors in inductive boost mode

2.2 THYRISTOR CONTROLLED PHASE ANGLE REGULATOR

Phase Angle Regulators are able to solve problems referred to the transmission angle which cannot be handled by the other series compensators. Even though these regulators, based on the classical arrangement of tap-changing transformers, are not able to supply or absorb reactive power they are capable of exchanging active power with the power system. Additionally, modern voltage and phase angle regulators are used to improve the transient stability, to provide power oscillation damping and to minimize the post-disturbance overloads and the corresponding voltage dips.

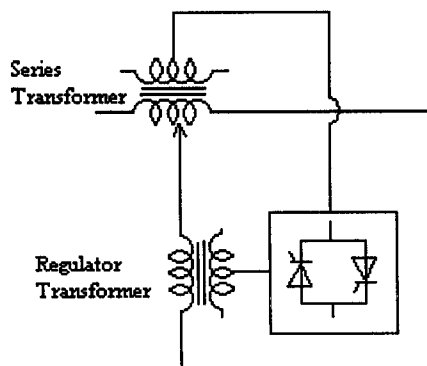


Figure 2.4 TCPAR

TCPAR is a phase shifting transformer adjusted by thyristor switches to provide a rapidly variable phase angle. In general, phasor shifting is obtained by adding a perpendicular voltage vector in series with a phase. This vector is derived from the other two phase's via-shunt connected transformers. The perpendicular series voltage is made variable with a variety of power electronics topologies. A circuit concept that can handle voltage reversal can provide phase shift in either direction. TCPAR can influence a flat change of phase angle. The phase shift is accomplished by adding or subtracting a variable voltage component that is perpendicular to the phase voltage of the line. This perpendicular voltage component is obtained from a transformer connected between other two phases. The attributes of these devices are the power control damping of oscillations and transient stability.

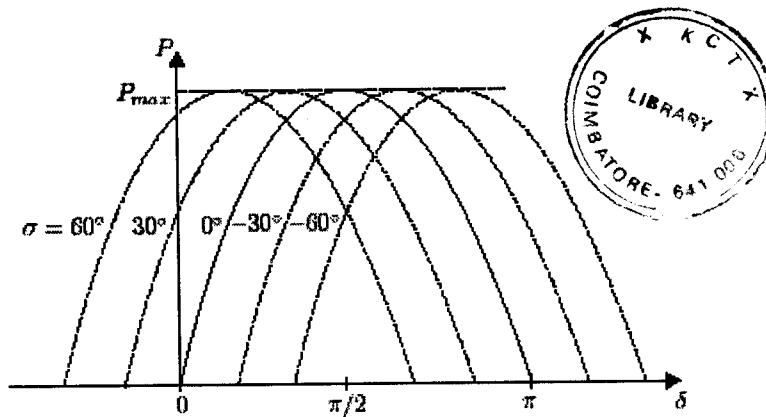


Figure 2.5 Transmitted power versus angle characteristics for a Phase Angle Regulator

To investigate the influence of a change in σ on the change of transmitted active Power P at different values of P , the derivative of with respect to σ is taken

$$\frac{\partial p}{\partial \sigma} = \frac{U_1 U_2}{X} \cos(\delta + \sigma) = \frac{U_1 U_2}{X} \sqrt{1 - \sin^2(\delta + \sigma)} \quad (2.5)$$

$$= \sqrt{\left(\frac{U_1 U_2}{X}\right)^2 - p^2} \quad (2.6)$$

From this and the assumption that $U_1 U_2 / X$ is constant the graphic in Figure 2.6 is drawn.

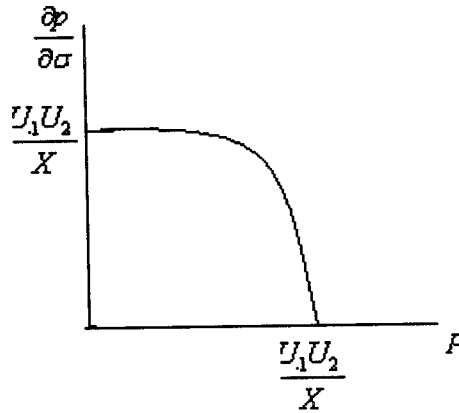


Figure 2.6 $\partial P / \partial \sigma$ versus p

This shows that for larger P the influence of a change in σ is rather small compared to the influence for a low transmitted active power.

2.3 UNIFIED POWER FLOW CONTROL

The unified power flow controller (UPFC) is a new device in FACTS family which consists of series and shunt connected converters. The unified power flow controller (UPFC) can provide the necessary functional flexibility for optimal power flow control. This approach allows the combined application of phase angle control with controlled series and shunt reactive compensation. Also, the real-time transition from one selection compensation mode into another mode for handling particular system conditions in an optimum manner is attainable.

It employs voltage-sourced inverters (i.e. inverters fed from a DC voltage source), composed of gate-turn off (GTO) thyristor valves, in appropriate harmonic neutralized configurations which ensure almost distortion-free output, economic manufacturing, and inherent redundancy for multilevel partial availability.

The proposed implementation of the unified power flow controller, using two voltage-sourced inverters operated from a common DC link capacitor, is shown schematically in Fig This arrangement is actually a practical realization of an AC to AC power converter with independently controllable input and output parameters Inverter 2 is used in the arrangement shown to generate voltage $V_{pq}(t)=V_{pq}\sin(\omega t-\phi_{pq})$ at the fundamental frequency ω with variable amplitude ($0 \leq V_{pq} \leq V_{pqmax}$) and phase angle ($0 \leq \phi_{pq} \leq 2\pi$), which is added to the AC system terminal voltage $V_0(t)$ by the series-connected coupling (or injection) transformer. With these stipulations, the inverter output voltage injected in series with the line can be used for direct voltage control, series compensation, and phase-shift, as discussed in the previous section.

The inverter output voltage injected in series with the line acts essentially as an AC voltage source. The current flowing through the injected voltage source is the transmission line current and it is a function of the transmitted electric power and the impedance of the transmission line.

The VA rating of the injected voltage source (i.e. that of Inverter 2) is determined by the product of the maximum injected voltage and the maximum line current at which power-flow control is still provided. This total VA is made up of two components: one is the maximum real power determined by the maximum line current and the component of the maximum injected voltage that is in phase with this current, and the other one is the maximum reactive power determined by the maximum line current and the component of the maximum injected voltage that is in quadrature with this current.

As known, the voltage-sourced inverter used in the implementation, can internally generate or absorb at its AC terminal all the reactive power demanded by the voltage/impedance/phase-angle control applied and only the real power demand has to be supplied at its DC input terminal. Inverter 1 (connected in shunt with the AC power system via a coupling transformer) is used primarily to provide the real power demand of Inverter 2 at the common DC link terminal from the AC power system. Since Inverter 1 can also

generate or absorb reactive power at its AC terminal, independently of the real power it transfers to (or from) the DC terminal, it follows that, with proper controls, it can also fulfill the function of an independent advanced static VAR compensator providing reactive power compensation for the transmission line and thus executing an indirect voltage regulation at the input terminal of the unified power-flow controller.

Although the power circuit configuration of the two inverters, linked by the common DC capacitor in the unified power-flow controller, can be similar, their requirements are different. Inverter 1 supplies real power to the DC link capacitor (to meet the demand of Inverter 2) and provides shunt reactive compensation for the transmission line. The flow of real power in or out of the DC link capacitor is controlled by the real power exchange between the inverter and the AC power system. If it is positive, the inverter generates reactive power for the AC system, and if it is negative, the inverter absorbs reactive power from the AC system. The difference voltage needed for full VAR output is determined mostly by the leakage impedance of the coupling transformer;. Inverter 2 injects the desired AC voltage in series with the line for power-flow control.

Assume that the voltage source (V) in series with the line can be controlled without restrictions. That is, the phase angle of pharos V can be chosen independently of the line current between 0 and 2π , and its magnitude is variable between zero and a defined, maximum value, V_{pqmax} . This implies that voltage source V_{pq} , must be able to generate and absorb both real and reactive power.

The reactive current source 1, is assumed to be either capacitive or inductive with a variable magnitude ($0 < I, < I_{pqmax}$) that is independent of the terminal voltage. To investigate the basic characteristics of the generalized power-flow controller, assume that its input terminal M is connected to the generator (V_s) via a transmission line-segment (X_L) and the magnitude V'_0 of voltage pharos at this terminal is kept constant by the reactive current source I_r . Voltage V'_0 and impedance X_L may be different from V ,

and $X/2$; that is, in the present model, the power flow controller is not necessarily located at the mid-point of the line. The voltage V_0 pharos, at the output terminal of the power-flow controller is assumed to be again the reference pharos ($V_0 = V_0'$) it is given by $V_0 = V_0' - V_{pq}$. A constant current I , determined by the receiving-end part of the power system, is assumed to be drawn from the output terminal of the power-flow controller.

Power flow control is achieved by adding voltage pharos V_{pq} , to terminal voltage pharos V_0 . Since pharos V_{pq} is stipulated to have no angular restrictions, and its magnitude is variable between 0 and V_{pqmax} its endpoint can be anywhere inside a circle with a radius of V_{pqmax} , whose centre is at the end of reference pharos V_0 , as shown in Figure 2.8(a). This means that by the appropriate definition (control) of pharos V_{pq} , the generalized power flow.

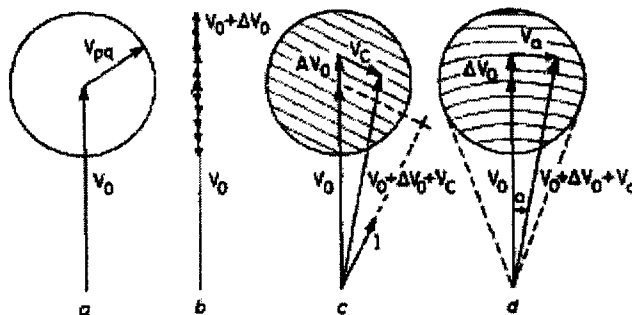


Figure 2.7. Phasor diagrams illustrating the operation of the unified power-flow controller when (a) controlling terminal voltage magnitude and phase angle, (b) regulating terminal voltage, (c) regulating terminal voltage and line impedance, and (d) regulating terminal voltage and phase angle

Controller can be used to accomplish different objectives:

Dedicated terminal voltage regulation or control, which is obtained simply by keeping the angle of V_{pq} zero (i.e. $V_{pq} = \pm \Delta V_0 = \pm \Delta V'_0$) and thus changing only the magnitude V , with respect to that of V_0 (or vice versa). Combined series line compensation and terminal voltage control, which is obtained by defining V_{pq} as a sum of voltage phasors V_c and ΔV_0 ; that is, $V_{pq} = V_c + \Delta V_0$.

Where phasor V_c is perpendicular to line current I and ΔV_0 is in phase with the terminal voltage phasor V_0 . Voltage V_c decreases or increases the effective voltage drop across the line segment impedance X , according to whether V lags or leads I . Combined phase angle regulation and terminal voltage control, which is obtained by defining V_{pq} as a sum of V_α and ΔV_0 that is, $V_{pq} = V_\alpha + \Delta V_0$

Where

$$V_\alpha = 2 V_0 \sin \alpha/2 \exp [\pm j(\pi/2 - \alpha/2)] \quad (2.7)$$

and ΔV_0 is again in phase with the terminal voltage V . The selected definition for phasor V_α ensures that the resultant terminal voltage phasor at the end of the line-segment, $V_0 = V'_0$ has the same magnitude as $V_0 + \Delta V_0$ i.e. ($|V_0 + \Delta V_0 + V_\alpha| = |V_0 + \Delta V_0| = V_0 \pm \Delta V_0$), but its phase angle is different from that of V , by α , as illustrated in Figure 2.9. In practical terms this means that phase shifting is achieved without any unintentional magnitude change in the controlled terminal voltage.

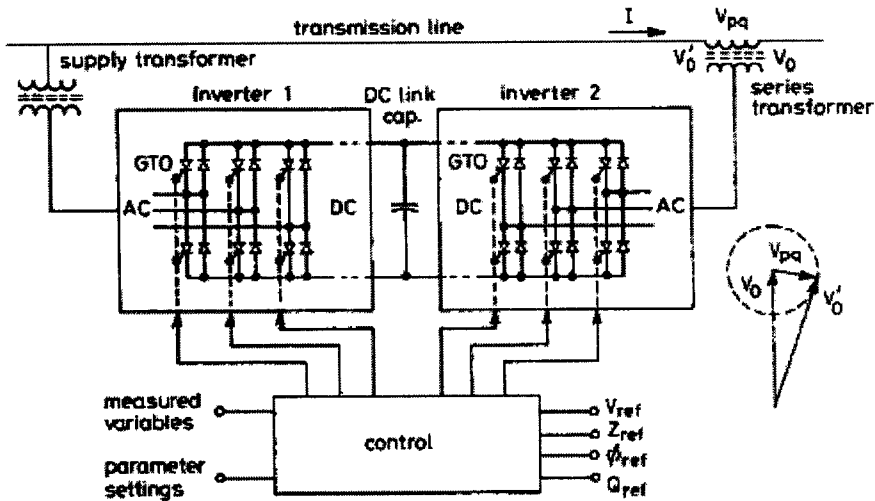


Figure 2.8 Implementation of the unified power-flow controller using two voltage-source inverters with a direct voltage link

FACTS devices will be used in interconnected power systems, and control compatibility and co-ordination may have to be maintained in the face of equipment failures and system changes. The approach would also provide considerable operating flexibility by its inherent adaptability to power system expansions and changes without any hardware alteration.

CHAPTER 3

COORDINATION OF POWER FLOW CONTROL WITH SEVERAL FACTS DEVICES

3.1 BASIC PRINCIPLES OF POWER FLOW CONTROL WITH FACTS DEVICES

3.1.1 Steady-State Models of FACTS Devices

It is well known that power flow control has three basic types:

Series compensation, parallel compensation, and phase-angle shifting. They can operate separately or jointly. The most typical control device is UPFC. It can control all the basic parameters of the system, i.e., bus voltage, line impedance and phase angle. Therefore, the UPFC model described in Fig can be taken as the unified model of different FACTS devices. When only the series or shunt branch of this model is taken, it simulates TCSC or STATCON. When both two branches are included, it can simulate TCPS or UPFC itself.

3.1.2. Power Flow Control Range with FACTS Device

Any controller should be robust, therefore, control variables of FACTS devices should vary in somewhat wide range to meet this requirement. When control variable of FACTS device varies, power flow on transmission line will change accordingly. However, because the controllability of shunt control, such as STATCON, is weaker than that of series control, in this paper, discussions will be focused on the controllability of the latter, such as TCSC, TCPR and UPFC.

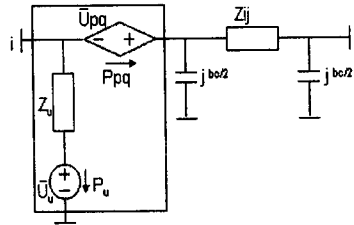


Figure 3.1 The unified model of FACTS devices in steady state

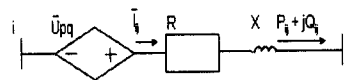


Figure 3.2 Model of the transmission line i-j installed with a FACTS device.

As shown in figure, the series voltage source U_{pq} is used to represent the series control. We assume

$$\bar{U}_i = U_i \angle 0 \text{ represents the series control.}$$

For simplicity, assume

$$U_i = U_i \angle 0, U_j = U_j \angle (-\theta), Z = R + jX \tag{3.1}$$

The power flow on such a compensated line can be written as

$$S_{ij} = p_{ij} + jQ_{ij} = U_j [(U_i + U_{pq} - U_j) / Z]^* \tag{3.2}$$

If $U_{pq} = 0$, the line is uncompensated And the power flow on it is

$$S_{ij} = S_{ij}^0 = P_{ij}^0 + jQ_{ij}^0 = U_j [(U_i - U_j) / Z]^* \tag{3.3}$$

From the above equations it can be obtained due to the FACT devices

$$S_{ij} = U_j [(U_i - U_j) / Z]^* + U_j u_{pq}^* / Z^* \tag{3.4}$$

3.2 14 BUS SYSTEM

A 14 bus system incorporating FACTS devices is shown for which the power flow solutions are found and to which GA is implemented for optimization.

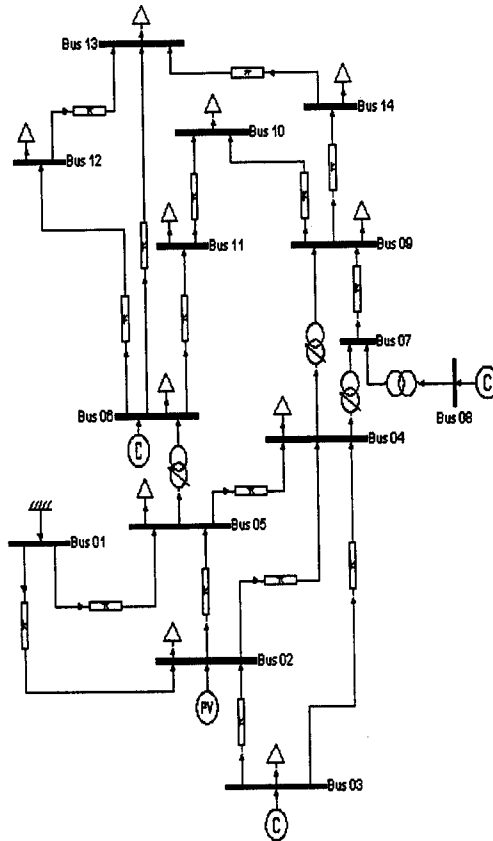


Figure3.3 14 bus system

3.3 UNIFIED POWER FLOW CONTROLLER

There are a number of feasible solid-state implementations for the unified power-flow controller described above. The implementation considered feasible and economical with presently available power semiconductors is akin to those proposed for the advanced static VAR compensator, controllable series compensator, and phase shifter.

Inverter 1 supplies real power to the DC link capacitor (to meet the demand of Inverter 2) and provides shunt reactive compensation for the transmission line. The flow of real power in or out of the DC link capacitor is controlled by the real power exchange between the inverter and the AC power system. This real power exchange is governed by the phase angle between the inverter and the AC system voltages. By contrast, the reactive power exchange, resulting from the line compensation, is determined by the amplitude difference between the inverter and AC system voltages. If this difference is zero (the inverter voltage has the same amplitude as the system voltage), the reactive power exchange is also zero; if it is positive, the inverter generates reactive power for the AC system, and if it is negative, the inverter absorbs reactive power from the AC system.

The difference voltage needed for full VAR output is determined mostly by the leakage impedance of the coupling transformer; it is typically not more than 15% of the nominal system voltage. Thus, to control the real and reactive powers independently, the nominal DC link voltage would have to be high enough to generate the AC output voltage of Inverter 1 with maximum amplitude which is about 15% higher than that of the AC system voltage at the secondary side of the coupling transformer. Inverter 2 injects the desired AC voltage in series with the line for power-flow control. In general, the phase angle of the injected voltage determines the mode of power flow control (transmission line voltage, impedance, or angle), and the amplitude defines to what extent it is applied.

Thus, the amplitude of the output voltage generated by Inverter 2 must be controllable from zero to a maximum determined by the rating of the power-flow controller. The real and reactive powers exchanged at the AC output of Inverter 2 are consequences of the voltage injection and are not directly Controllable; the ratio between real and reactive power is determined strictly by the relative phase angle between the injected voltage and the line current. The internal control of the solid-state power-flow controller (to be published at a later date) is structured so as to accept externally derived reference signals, in an order of selected priority, for the desired reactive shunt compensation, series compensation, transmission angle, and terminal voltage.

These reference signals are used in closed control loops to force the inverters to produce the AC voltages (which correspond to the appropriate combination of the reference signals) at the input (shunt-connected) and output (series-connected) terminals of the power-flow controller, and thereby establish the transmission parameters desired. The control also maintains the necessary DC link voltage and ensures smooth real power transfer between the two inverters

For UPFC, the series voltage source voltage source can insert a voltage of arbitrary magnitude and phase. In practice, $U_{pq} = U_{pq} \angle \gamma$ where $0 \leq \gamma \leq 360^\circ$, $0 \leq U_{pq} \leq U_{pq \max}$. Equation (3.3) describes a circle with centre at S_{ij} (initial power flow on the uncompensated line) and a radius of $[\bar{U}_j U_{pq}^* / Z^*]$

The allowable operation point for this UPFC is wherever within this circle. Obviously, the change of line power flow is dictated by the initial operation conditions and the magnitude of this additional voltage source. Note that to decrease the line power flow to zero with UPFC by this way is essential different from the opening of this line, because in the first case the charging power (current) on this line still exists.

While the reliability of the network in this line still exists, while the reliability of the network in this case is also higher.

$0 \leq U_{pq} \leq U_{pq \max}$, $U_{pq} = U_{pq} \angle (\pm\pi/2)$. The additional power S_{ij}^{facts} on this line will be

$$S_{ij}^{\text{facts}} = P_{ij}^{\text{facts}} + jQ_{ij}^{\text{facts}} = U_{pq} U_j (a + jb) e^{\pm j\pi/2} \quad (3.5)$$

Where

$$a = (R \cos \theta + X \sin \theta) / (R^2 + X^2) \quad (3.6)$$

$$b = (X \cos \theta - R \sin \theta) / (R^2 + X^2) \quad (3.7)$$

In high voltage transmission system, $R \ll X$, $0 < \theta < 20^\circ$, hence $a > 0$, $b < 0$. In such case,

a) if $y = \pi/2$,

$$Q_{ij}^{\text{facts}} / P_{ij}^{\text{facts}} = (-a) / b < 0 \quad (3.8)$$

b) if $y = -\pi/2$,

$$Q_{ij}^{\text{facts}} / P_{ij}^{\text{facts}} = a / (-b) < 0 \quad (3.9)$$

The above two equations describe a straight line with its slope being negative. Because R/X ratio is small, the slope is very small. When U_{pq} varies from 0 to $U_{pq \max}$, The allowable range for TCPR is a straight line, i.e., the diameter of the corresponding UPFC circle. If the controller is a TCSC, then $\overline{U}_{pq} = jX_c I_{ij}^*$. The power flow will be

$$\overline{S}_{ij} = \overline{S}_{ij}^0 + \overline{U}_j (-jX_c I_{ij}^*) / Z^* \quad (3.10)$$

But

$$\overline{S}_{ij} = \overline{U}_j I_{ij}^*, \text{ so } \overline{S}_{ij} = \overline{S}_{ij}^0 / (Z^* + jX_c) \quad (3.11)$$

$$\overline{S}_{ij} - \overline{S}_{ij}^0 Z^* / 2R = (\overline{S}_{ij}^0 Z^* / 2R) \{ [R - j(X_c - X)] / [R + j(X_c - X)] \}. \quad (3.12)$$

When X_c in the above equation varies from $-\infty$ to ∞ , this equation describes a circle on P-Q plane with its center at $\overline{S}_{ij}^0 Z^* / 2R$ and a radius of $\left| \overline{S}_{ij}^0 Z^* / 2R \right|$. This circle passes through the original and the initial operating point \overline{S}_{ij}^0 .

3.4 THYRISTOR-CONTROLLED SERIES COMPENSATOR

Thyristor-controlled series compensators (TCSC) are connected in series with the lines. The effect of a TCSC on the network can be seen as a controllable reactance inserted in the related transmission line that compensates for the inductive reactance of the line. This reduces the transfer reactance between the buses to which the line is connected. This leads to an increase in the maximum power that can be transferred on that line in addition to a reduction in the effective reactive power losses. The series capacitors also contribute to an improvement in the voltage profiles. Figure shows a model of a transmission line with a TCSC connected between buses i and j. The transmission line is represented by its lumped π -equivalent parameters connected between the two buses. During the steady state, the TCSC can be considered as a static reactance $-jX_c$. This controllable reactance, X_c , is directly used as the control variable to be implemented in the power flow equation

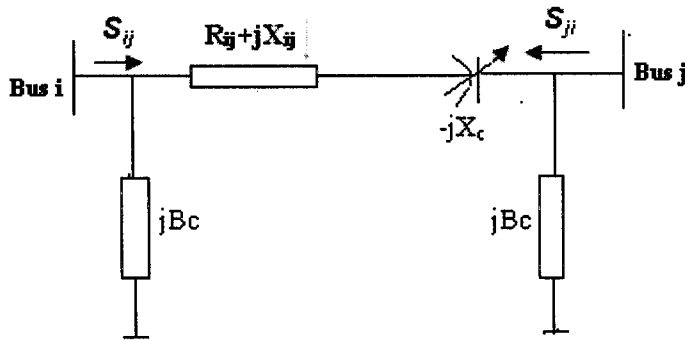


Figure3.4 Model of a TCSC

Let the complex voltages at bus i and bus j be denoted as $V_i^* \delta_i$ and $V_j^* \delta_j$, respectively.

The complex power flowing from bus i to bus j can be expressed as

$$S_{ij}^* = P_{ij} - jQ_{ij} = V_{ij}^* \quad (3.13)$$

$$= V_i^* [(V_i - V_j)Y_{ij} = V_i(jB_c)] \quad (3.14)$$

$$= V_i^2 [G_{ij} + j(B_{ij} + B_c)] - V_j^* (G_{ij} + B_{ij}) \quad (3.15)$$

Where

$$G_{ij} + jB_{ij} = 1/(R_L + jX_L - jX_c) \quad (3.16)$$

Equating the real and imaginary parts of the above equations, the expressions for real and reactive power flows can be written as

$$P_{ij} = V_i^2 G_{ij} - V_i V_j G_{ij} \cos(\delta_i - \delta_j) - V_i V_j B_{ij} \sin(\delta_i - \delta_j) \quad (3.17)$$

$$Q_{ij} = -V_i^2 (B_{ij} + B_c) + V_i V_j G_{ij} \sin(\delta_i - \delta_j) + V_i V_j B_{ij} \cos(\delta_i - \delta_j) \quad (3.18)$$

Similarly, the real and reactive power flows from bus j to bus i can be expressed as

$$P_{ji} = V_j^2 G_{ij} - V_i V_j G_{ij} \cos(\delta_i - \delta_j) - V_i V_j B_{ij} \sin(\delta_i - \delta_j) \quad (3.19)$$

$$Q_{ij} = -V_j^2 (B_{ij} + B_c) + V_i V_j G_{ij} \sin(\delta_i - \delta_j) + V_i V_j B_{ij} \cos(\delta_i - \delta_j) \quad (3.20)$$

The active and reactive power loss in the line can be calculated as

$$P_L = P_{ij} + P_{ji} \quad (3.21)$$

$$= V_i^2 G_{ij} + V_j^2 G_{ij} - 2V_i V_j G_{ij} \cos(\delta_i - \delta_j) \quad (3.22)$$

$$Q_L = Q_{ij} + Q_{ji} \quad (3.23)$$

$$= -V_i^2 (B_{ij} + B_c) - V_j^2 (B_{ij} + B_c) + 2V_i V_j B_{ij} \cos(\delta_i - \delta_j) \quad (3.24)$$

These equations are used to model the TCSC in the OPF formulations

3.5 THYRISTOR-CONTROLLED PHASE ANGLE REGULATOR

In a thyristor-controlled phase angle regulator, the phase shift is achieved by introducing a variable voltage component in perpendicular to the phase voltage of the line. The static model of a TCPAR having a complex tap ratio of $1: \alpha$ and a transmission line between bus i and bus j is shown in Figure

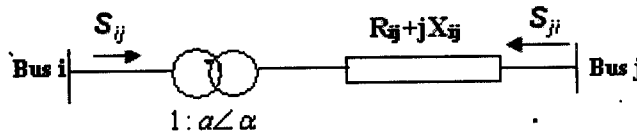


Figure 3.5 Model of TCPAR

The real and reactive power flows from bus i to bus j can be expressed as

$$P_{ij} = \text{Re}\{V_i^* [(a^2 V_i - a^* V_j) Y_{ij}]\} \quad (3.25)$$

$$= -a^2 V_i^2 G_{ij} - a V_i V_j B_{ij} \cos(\delta_i - \delta_j + \alpha) - a V_i V_j G_{ij} \sin(\delta_i - \delta_j + \alpha) \quad (3.25)$$

And
$$Q_{ij} = -\text{Im}\{V_i^*[(a^2V_i - a^*V_i)Y_{ij}]\} \quad (3.26)$$

$$= -a^2V_i^2G_{ij} - aV_iV_jB_{ij} \cos(\delta_i - \delta_j + \alpha) - aV_iV_jG_{ij} \sin(\delta_i - \delta_j + \alpha) \quad (3.27)$$

Similarly, real and reactive power flows from bus j to bus i can be written as

$$P_{ji} = \text{Re}\{V_j^*[(V_j - aV_j)Y_{ij}]\} \quad (3.28)$$

$$= V_j^2G_{ij} - aV_iV_jG_{ij} \cos(\delta_i - \delta_j + \alpha) - aV_iV_jB_{ij} \sin(\delta_i - \delta_j + \alpha) \quad (3.29)$$

And

$$Q_{ji} = -\text{Im}\{V_j^*[(V_j - aV_j)Y_{ij}]\} \quad (3.30)$$

$$= -V_j^2B_{ij} + aV_iV_jB_{ij} \cos(\delta_i - \delta_j + \alpha) + aV_iV_jG_{ij} \sin(\delta_i - \delta_j + \alpha) \quad (3.31)$$

The real and reactive power loss in the line having a TCPAR can be expressed as

$$P_l = P_{ij} + P_{ji} \quad (3.32)$$

$$= a^2V_i^2G_{ij} + V_j^2G_{ij} - 2V_iV_jG_{ij} \cos(\delta_i - \delta_j + \alpha) \quad (3.33)$$

$$Q_l = Q_{ij} + Q_{ji} \quad (3.34)$$

$$= -a^2V_i^2B_{ij} - V_j^2B_{ij} + 2V_iV_jB_{ij} \cos(\delta_i - \delta_j + \alpha) \quad (3.35)$$

This mathematical model makes the Y-bus asymmetrical. In order to make the Y-bus symmetrical, the TCPAR can be simulated by augmenting the existing line with additional power injections at the two buses. The injected active and reactive powers at bus i (ΔP_i , ΔQ_i) and bus j (ΔP_j , ΔQ_j) are given as

$$\Delta P_i = -a^2V_i^2G_{ij} - aV_iV_j[G_{ij} \sin(\delta_i - \delta_j) - B_{ij} \cos(\delta_i - \delta_j)] \quad (3.36)$$

$$\Delta P_j = -aV_iV_j[G_{ij} \sin(\delta_i - \delta_j) + B_{ij} \cos(\delta_i - \delta_j)] \quad (3.37)$$

$$\Delta Q_i = a^2V_i^2B_{ij} + aV_iV_j[G_{ij} \cos(\delta_i - \delta_j) - B_{ij} \sin(\delta_i - \delta_j)] \quad (3.38)$$

$$\Delta Q_j = -aV_iV_j[G_{ij} \cos(\delta_i - \delta_j) - B_{ij} \sin(\delta_i - \delta_j)] \quad (3.39)$$

3.6 POWER FLOW CONTROL RANGES

In Figure Control ranges of different FACTS devices are depicted. In which the area of the circle is the control range of UPFC; the diameter of which is the control range of TCPR; the solid portion of the dotted circle is that of TCSC. Figure3.6 shows the initial operating point is close to the origin. Figure3.7 shows the initial operating point is far away from the origin. From Figure3.7. It can be observed the power flow control range of UPFC is superior to TCPR or TCSC. TCSC provides larger control range than TCPR

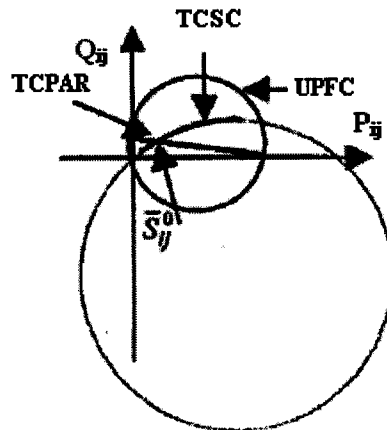


Figure3.6 S_{ij} close to the origin (0,0)

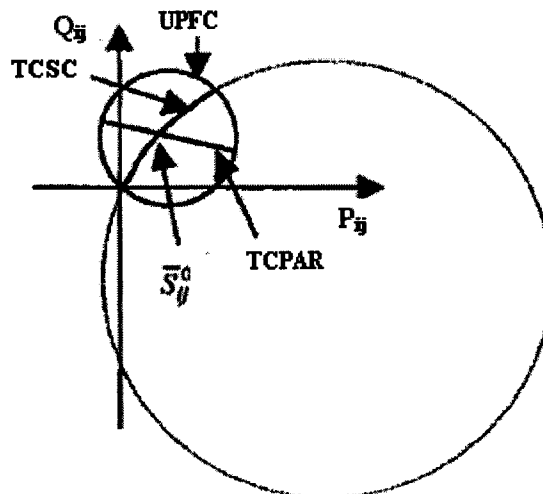


Figure3.7 S_{ij} far away from origin

Power flow control range of FACTS devices

CHAPTER 4

GENETIC ALGORITHM

4.1 INTRODUCTION TO GENETIC ALGORITHM

GA's are usually more flexible and robust, and they have been successfully used in power system planning, so, in this paper Genetic Algorithm is selected to solve this problem. Genetic algorithms are essentially search algorithms based on the mechanics of nature (e.g., natural selection, survival of the fittest) and natural genetics. They combine solution evaluation with randomized, structured exchanges of information between solutions to obtain optimality. Genetic algorithms are considered to be the robust methods because no restrictions on the solution space are made during the process. The power of this algorithm comes from its ability to exploit historical information structures from previous solution guesses in an attempt to increase the performance of future solution structures.

GAs evaluate encodings of the original parameters instead of the original parameters instead of the actual parameters. The parameter set is reduced to a series of representative symbols from an arbitrary yet effective alphabet and solutions are evaluated based on certain symbol structures. GAs maintain a population of solution structures throughout the process, therefore they are not limited by the selection of initial single point solution guesses. In this way the entire solution space may be considered and multiple solutions detected. GAs incorporate probabilistic transition rules rather than simple deterministic rules. The programmer only has to define the objective function and the encoding technique.

4.2 SOLUTION MODELING

GA algorithms borrow the analogous biological terms for each step. GAs maintain a population of parameter set solutions and iterate on the complete population. Each iteration is called as the generation. The problem parameter set include its environment inputs and output is represented by a fixed length string of symbols, usually from the binary alphabet $\{0, 1\}$. The string called a chromosome represent a single solution point in the problem space. The chromosome string consists of genetic material in specific locations called as loci. Each location contains a symbol or series of symbols called genes, which assume values, called alleles.

Evaluation of the chromosomes string is accomplished by decoding the encoded symbols and calculating the objective function for the problem using the decoded parameter set. The result of the objective function calculation is used to calculate the value of the string with respect to all other chromosomes string within the population. This raw value measure is called the string fitness value and can be calculated in any number of ways based on the goal of ways based on the goal of the optimization. For the goal of the optimization.

For maximization problem the fitness value could assume the value of the objective function or pay off cost itself .For minimization problems, a folding function could be used. Representation of the problem parameter set is important. The encoding must be designed to utilize the algorithm ability to transfer information between chromosome strings efficiently and effectively. GA is essentially derived from a simple model of population genetics. The three prime operators associated with the GA are reproduction, crossover and mutation.

Reproduction is simply an operation whereby an old chromosome is copied into a “mating pool” according to its fitness value. More highly fitted chromosome (with better value of the objective function) receives a higher number of

copies in the next generation. Copying chromosomes according to their fitness value means that chromosomes with a higher value have a higher probability of contributing one or more offspring in the next generation.

Crossover is an extremely important component of the GA. It is a structured recombination operation. This operation is similar to two scientists exchanging information.

4.3 COORDINATION OF POWER FLOW CONTROL BASED ON GENETIC ALGORITHM

Much more complicated is the power flow control in interconnected system with several FACTS devices. Here the coordination of more than one power flow controller becomes the kernel point. Especially for the opening of electric energy market, the maximal power that can be transmitted via a transmission line or a set of transmission lines is of ultimate importance. Obviously, this problem can be described as an optimization problem with the objective of maximizing the active power flowing on one line or the total active power flowing on a set of lines, subjected to those physical and operational constraints of the system.

However, because the participation of FACTS devices, this problem is not only nonlinear, but may also be non-smooth and non-convex. For such a problem conventional gradient-based methods are mostly no longer efficient. Based on the mechanism of natural selection and natural genetics, genetic algorithms (GA's) seem to be the promising candidates for this purpose. Without any derivation and no need of other auxiliary knowledge, these algorithms use fitness function to direct the search among a population of points and will converge to a global optimum with high probability.

Comparing with the conventional optimization methods, GA's are usually more flexible and robust, and they have been successfully used in power system planning. So, in this paper genetic algorithm is selected to solve this problem.

4.4 MODELING OF POWER FLOW CONTROL WITH FACTS DEVICES

The objective function and the corresponding constraints of this problem can be represented by

$$\text{Max } F = \sum_{i=1}^m P_i \quad (4.1)$$

$$\text{s.t } U_i^{\min} \leq U_i \leq U_i^{\max} \quad (4.2)$$

$$I_{ij}^{\min} \leq I_{ij} \leq I_{ij}^{\max} \quad (4.3)$$

$$U_{pqj}^{\min} \leq U_{pqj} \leq U_{pqj}^{\max} \quad (4.4)$$

$$0 \leq \gamma_i \leq 2\pi$$

$$Q_{ui}^{\min} \leq Q_{ui} \leq Q_{ui}^{\max} \quad (4.5)$$

$$P_{pq} = P_u \quad (4.6)$$

Where P_i is the active power transmitted via a line; m is the number of lines of lines in a transfer corridor; U_i is the magnitude of i node voltage; I_{ij} is the magnitude of i - j branch current; U_{pqj} , γ_i is the magnitude and phase angle of the series voltage source; P_{pq} and P_u is the active power of a series or shunt voltage source respectively. The value of γ and P_{pq} depend on the type of the FACTS device studied. The constraint is active only when UPFC is investigated. In addition, power flow control with FACTS devices must subject to the corresponding power flow equations. Assuming a FACTS device installed at node I on branch i - j corresponding power flow constraint can be expressed as follows;

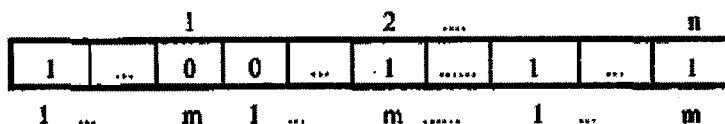
$$P_i = U_i \sum_{k \in i} U_k (G_{ik} \cos \theta_{ik} + B_{ik} \sin \theta_{ik}) + P_i^{\text{facts}} \quad (4.7)$$

$$Q_i = U_i \sum_{k \in i} U_k (G_{ik} \sin \theta_{ik} - B_{ik} \cos \theta_{ik}) + Q_i^{\text{facts}} \quad (4.8)$$

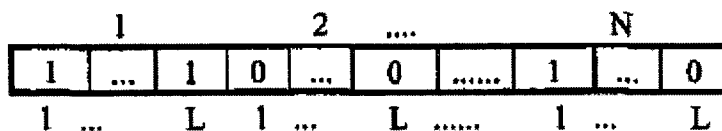
$$P_j = U_i \sum_{k \in i} U_k (G_{jk} \cos \theta_{jk} + B_{jk} \sin \theta_{jk}) + P_j^{facts} \quad (4.9)$$

$$Q_j = U_i \sum_{k \in i} U_k (G_{jk} \cos \theta_{jk} + B_{jk} \sin \theta_{jk}) + Q_j^{facts} \quad (4.10)$$

Where P_i facts, Q_i facts P_j facts Q_j facts are additional power on the i - j caused by the FACTS device



(a) Individual code string at genetic coordination stage



(b) Individual code string at genetic optimization stage

Figure 4.1 String structure for the coordination of power flow controllers: (a) individual code string a1 genetic coordination stage and (b) individual code string at genetic optimization stage.

It should be noted if the direction of the power flow on one or a set of transmission lines should be reversed, an independent optimization problem has to be solved

4.5 IMPROVED GENETIC ALGORITHM

To make GA applicable to the power flow control with FACTS devices, some important improvements of which should be made. These improvements as well as the basic procedure of this improved GA are described as follows:

4.5.1 Objective function

Owing to the fact that the constraints of this model are rather complicated, the method used in such an improved GA to handle these constraints differs from those of the conventional ones. They are directly incorporated in the objective function instead of

imposed upon the fitness function. Such a measure can avoid the shortcoming that different constraints have different effects on fitness function. Thus, the objective function used is

$$\text{MaxF} \sum_{l=1}^m P_l - \lambda_1 \sum_{i=1}^n |U_i - U_i^{\text{lim}}| - \lambda_2 \sum |I_{ij} - U_{ij}^{\text{lim}}| \quad (4.11)$$

Where λ is the penalty factor that can be modified during the optimization process, U_i^{lim} is the node voltage limit, I^{lim} is the line current limit. Commonly, GAs start with random generation of initial population which represent possible solutions of the problem. Then the fitness of each individual is evaluated and new populations are generated by genetic operators (Reproduction, Crossover and Mutation) until the maximal number of generation is reached.

4.5.2 Encoding

The objective is to find the optimal power flow solutions of various FACTS devices within the equality and inequality constrains. Each individual is represented by FACTS n number of strings, as shown in Figure where FACTS n is the number of FACTS devices needed to be analyzed in the power systems.

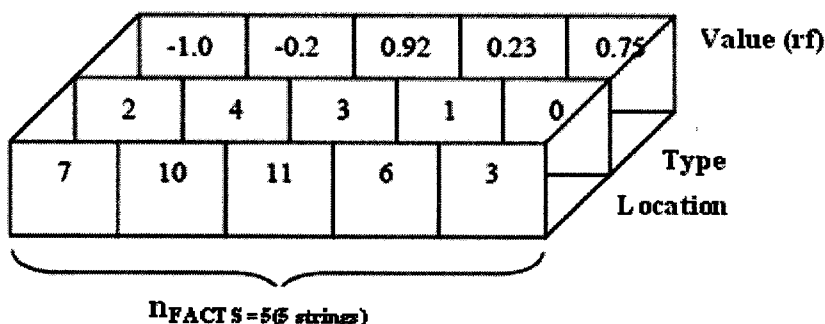


Figure 4.2. Individual configuration of FACTS devices

As shown in Figure the first value of each string corresponds to the location information. It is the number of the transmission line where the FACTS is to be

located. Each string has a different value of location .In other words, it must be ensured that on one transmission line there is only one FACTS device.

The second value represents the types of FACTS devices. The values assigned to FACTS devices are: 1 for TCSC; 2 for TCPST; 3 for UPFC, and 0 for no FACTS situation. Particularly, if there is no FACTS device needed on the transmission line, the value 0 will be employed. The last value rf represents the rated value of each FACTS device. This value varies continuously between -1 and $+1$.

4.5.3 Initial population

The initial population of strings is randomly selected from the binary-coded domain of control variables. Fig shows the string structure for the power flow control with FACTS devices. Where n is the number of FACTS devices; m is the state code of individual FACTS device; N represents the scope of the population; L is the length of each code segment. The initial population is distributed over the state space of control variables. To ensure the precision of computation, adequate hits should be taken for control variables. Such as, for UPFC, U_{pq} , γ , Q_u , take 5, 10, 5 binary-code bits respectively.

4.5.4 Statistics

The maximum fitness $F_{\max}(k)$, total fitness $F_{\Sigma}(k)$ and average fitness of certain generation $F_{\text{aver}}(k)$ are calculated, where k is the number of iterations. The initial population is generated by the following parameters:

n_{FACTS} : the number of FACTS devices to be located

n_{Type} : FACTS types

n_{Location} : the possible locations for FACTS devices

n_{Ind} : the number of individuals in a population

First, as shown in Figure a set of n_{FACTS} numbers of strings are produced. For each string, the first value is randomly chosen from the possible locations

$n_{Location}$. The second value, which represents the types of FACTS devices, is obtained by randomly drawing numbers among the selected devices. Particularly, after the optimization, if there is no FACTS device necessary on the transmission line, the second value will be set to zero. The third value of each string, which contains the rated values of the FACTS devices, is randomly selected between -1 and $+1$. To obtain the entire initial population, the above operations are repeated n_{Ind} times. Figure shows the calculation of the entire population.

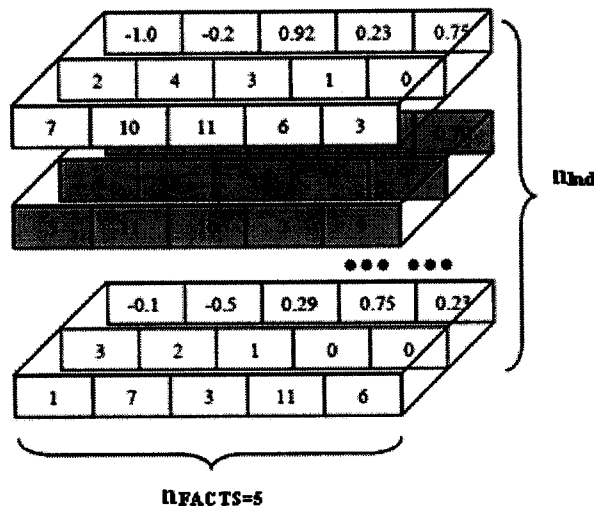


Figure4.3. Calculation of the entire population

4.5.5 Fitness calculation

After encoding, the objective function (fitness) will be evaluated for each individual of the population. The fitness is a measure of quality, which is used to compare different solutions. Then reproduction, crossover and mutation are applied successively to generate the offspring.

4.5.6 Reproduction

Reproduction is a process where the individual is selected to move to a new generation according to its fitness. The strings of the same number as the population size will be copied into a “mating pool” according to their fitness values. A simulated weighted roulette wheel is then used to select mates. Simulated N coin tosses on the roulette wheel select the corresponding number of mates.

This means each string in the “mating pool” will likely be mutated with variable mutation probability. If this number is less than the variable mutation probability, bits in the string will be changed from 1 to 0, or vice versa. Such a mutation operation produces a new string. Finally, strings in the “mating pool” are grouped into couples. Each string couple would swap their bits according to one-point crossover probability.

In the reproduction process, the fittest individual will be selected. In other words, the individual with a larger fitness has the higher probability of contribution to one or more offspring in the next generation. In this research, the roulette wheel selection method is employed. Each individual in the population has its interval. The size of each interval corresponds to the fitness of the individual and can be defined as

$$P_r = \frac{Fitness_r}{\sum_{i=1}^{n_{Ind}} Fitness_i} = \frac{Fitness_r}{Fitness_{sum}} \quad (4.12)$$

Where

n_{Ind} : the number of individuals in the population

Fitness : the fitness of the rth individual

p_r : the proportion of the rth individual on the roulette wheel

Sum Fitness : the sum of fitness of the population

To select an individual, a random number is generated in the interval $[0, 1]$ and the individual whose segment spans the random number is selected. The probability of an individual's reproduction is proportional to its fitness. A five individual example is shown in Figure. Individual 5 is the fittest individual and occupies the largest part in the roulette wheel. Therefore, it has higher probability of contribution to offspring in the next generation.

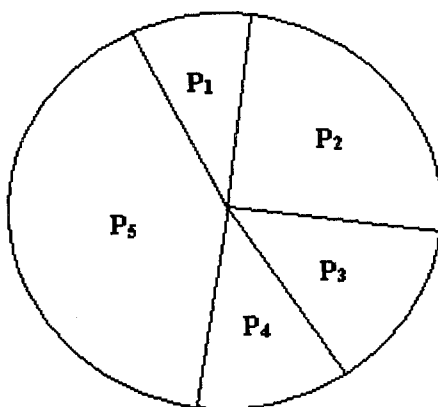


Figure 4.4. Roulette wheel selection

4.5.7 Crossover

After the process of reproduction, crossover is applied. The main objective of Crossover is to reorganize the information of two different individuals and produce a new one. This operator promotes the exploration of new regions in the search space. As shown in Figure a two-point crossover is applied and the probability of the crossover p_c is selected as 0.95. First, two crossing points are selected uniformly at random along the individuals. Elements outside these two points are kept to be part of the offspring. Then, from the first position of crossover to the second one, elements of the three strings of both individuals are exchanged. After crossover, the two individuals are shown in Figure 4.4 .

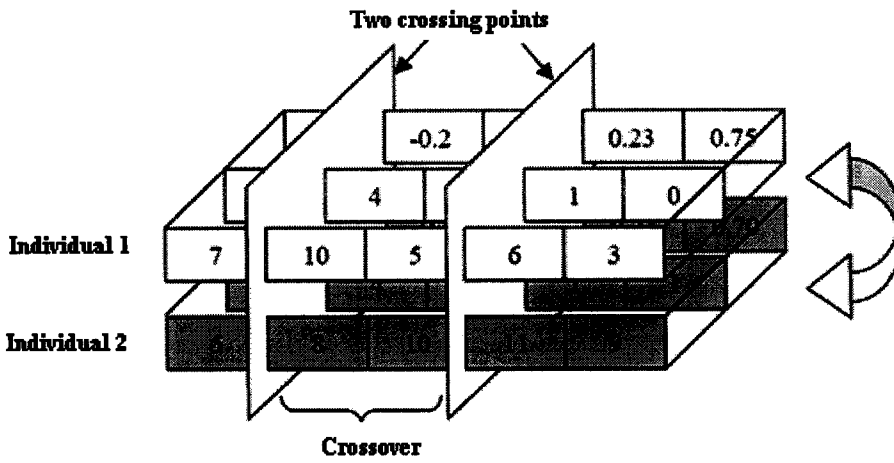


Figure 4.5. Individual

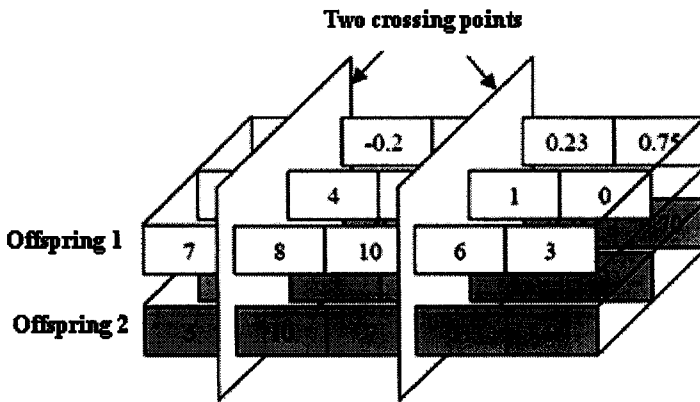


Figure 4.6. Offspring before correction

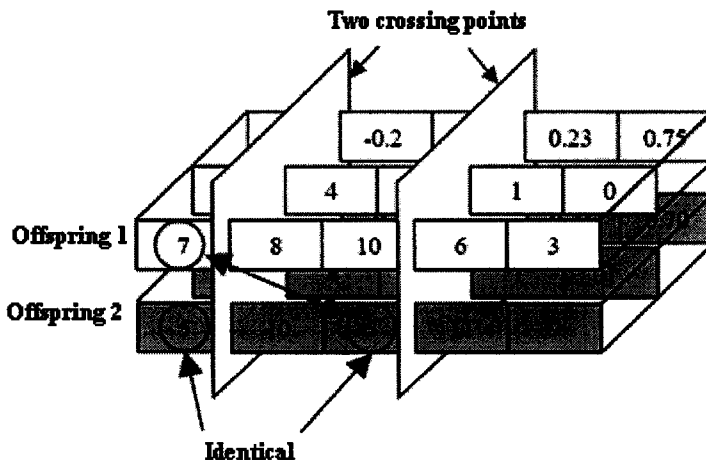


Figure 4.7. Offspring after correction

4.5.8 Mutation

In order to accelerate the convergence speed of GA, variable mutation probability is used to control the mutation of individual binary-coded string during iteration. This can accelerate mutation of individuals with small fitness values. The variable mutation probability is calculated by

$$p^i(k) = \begin{cases} pmf & \text{if } F_i \geq F_{aver} \\ pmf \left[1 + \exp\left(\frac{F_{aver} - F_i}{F_{aver}}\right) \exp(-k) \right] & \text{Otherwise} \end{cases} \quad (4.13)$$

Where P_{mf} is a fixed mutation probability of individual string, generally set as 0.001; k is the number of iterations; F_i is the value of objective function for individual at $(k-1)^{th}$ iteration; F_{aver} is the average value of objective function for population for $(k-1)^{th}$ iteration; $P^i(k)$ is the mutation probability of individual at k^{th} iteration.

After all the strings finish their mutation and crossover, a new generation is reproduced. Each string is then decoded back to the control variables for computing its fitness value. The statistics will compute the new maximum fitness, the total fitness and average fitness. The convergence condition is the fitness scores of five successive generations are same. If this condition is satisfied, the iteration process will be terminated. Otherwise, a new reproduction cycle will begin. The above-mentioned operations of selection, crossover and mutation will be repeated until the maximal number of generation is reached.

4.5.9 Flow chart of the GA optimization

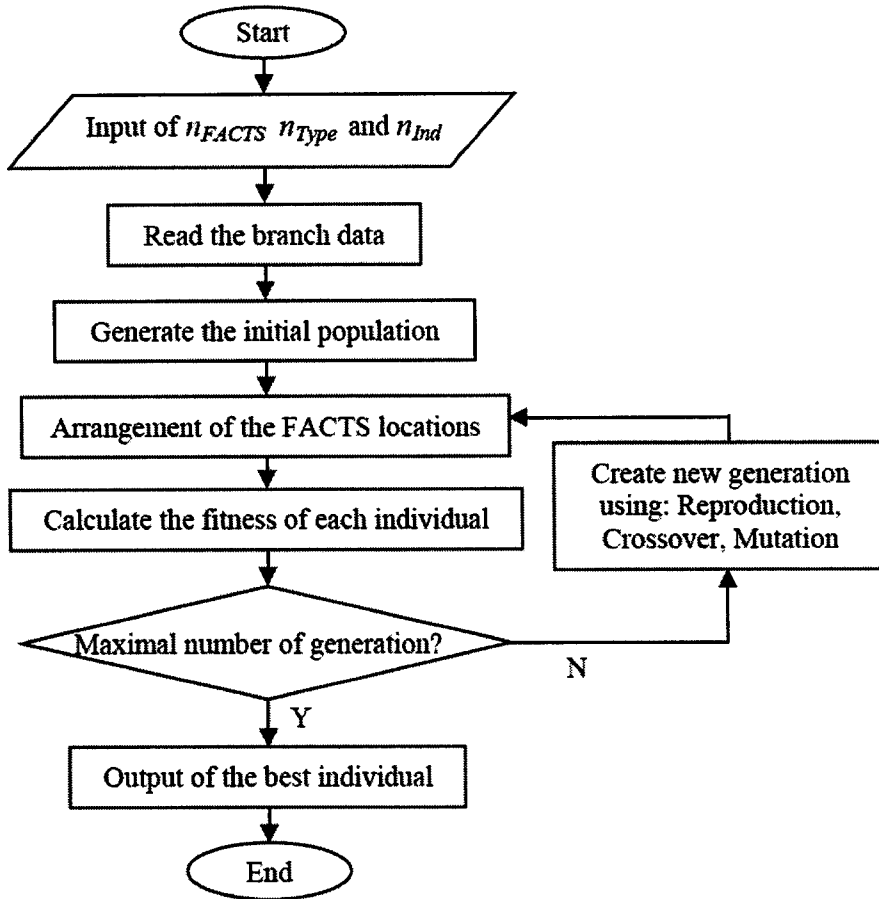


Figure4.8 Flowchart

CHAPTER 5

SIMULATED OUTPUT RESULTS

A MATLAB coding has been developed to optimize the power flow to reduce the error using improved Genetic Algorithm after incorporating the FACTS Devices in 14 bus system. Voltage profile at the buses has improved and the real and reactive power transfer is controlled and the power flow control ranges for these device in the 14 bus system are drawn. Coordination of power flow control performance for TCSC, TCPR and UPFC before and after optimization of power flow using improved Genetic Algorithm are shown. The MATLAB Codings generated are listed in APPENDIX 1.

5.1 TCSC OUTPUT RESULT

Simulated result for TCSC is shown here. TCSC is incorporated in transmission line and the power flow control ranges are found. A graph for real and reactive power before optimization is given below

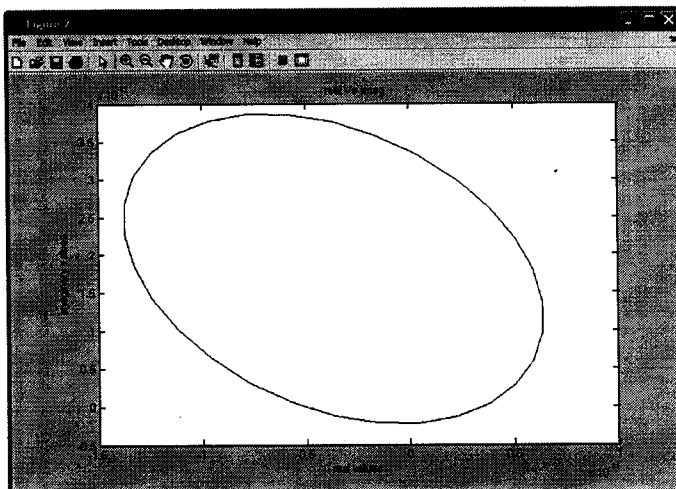


Figure 5.1. TCSC before optimization

Error minimizing

Genetic algorithm is implemented and the power flow control range is found and optimization of the power flow control range is made. The lower dotted line indicates the reference value and error is minimized for various points by considering the reference line which is shown below.

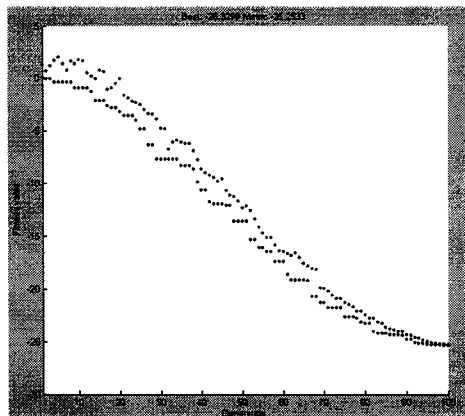


Figure 5.2.Error minimization

TCSC result after optimization

The optimized result after genetic algorithm implementation is shown below. Since TCSC works through the transmission system directly, it is much more effective than the shunt FACTS devices in the application of power flow control and power system oscillation damping control. The optimized result of power flow control range for TCSC is shown as below.

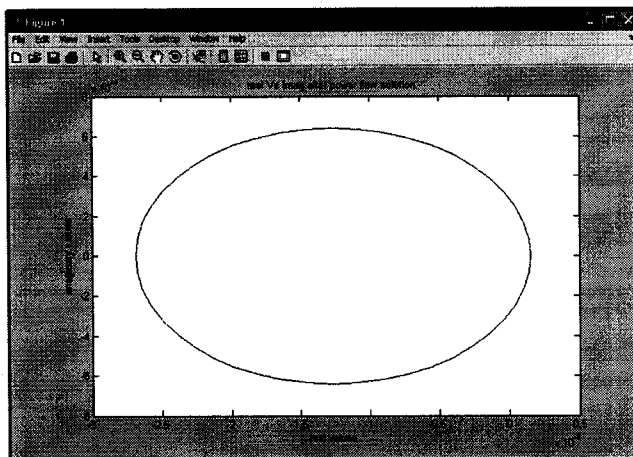


Figure 5.3. TCSC after optimization

5.2 TCPAR OUTPUT RESULTS

The graph which is shown below indicates the Modeling of TCPAR controller for real and reactive power.

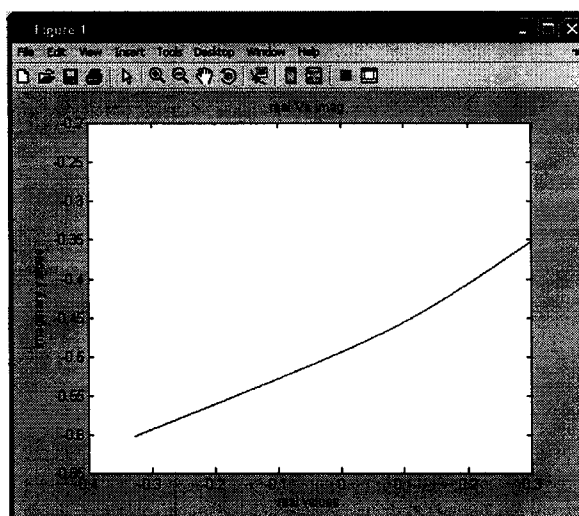


Figure 5.4. TCPAR before optimization

TCPAR after optimization

After modeling of this FACTS controller genetic algorithm is implemented and error is minimized by choosing a reference line. The phase angle is

regulated and the optimization of the power flow control range after genetic algorithm implementation is shown below

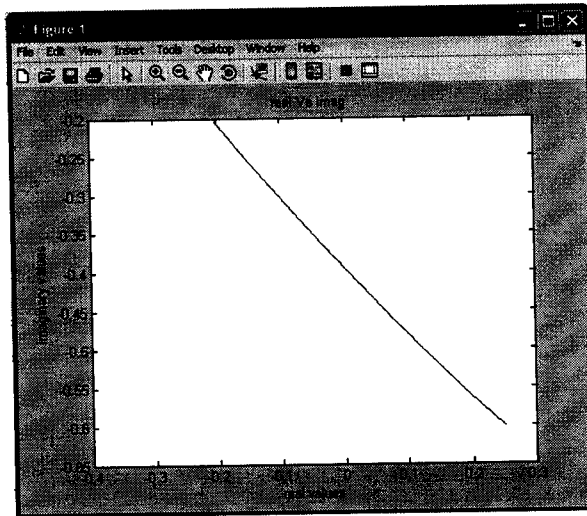


Figure 5.5.CPR after optimization

5.3 UPFC OUTPUT RESULT

The simulated output result before genetic algorithm implementation is shown. The graph for real and reactive power is drawn.

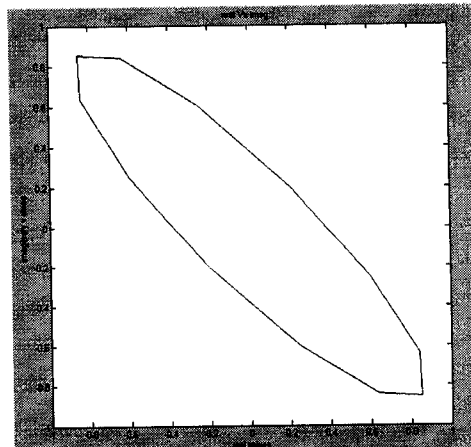


Figure 5.6.Before optimization

UPFC after optimization

. The UPFC is the most powerful and versatile FACTS device due to the facts that the Line impedance, terminal voltages, and the voltage angles can be controlled by it as well. Optimized result of power flow control range by incorporating UPFC in transmission line after genetic algorithm implementation is shown

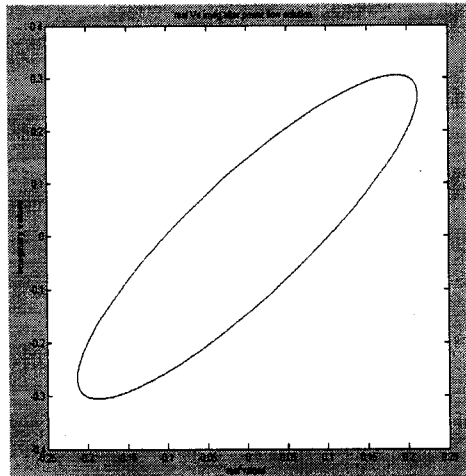


Figure 5.7.UPFC after optimization

A comparison of power flows in different control modes shows that the controllability of power flow is dependent on the number of FACTS devices installed in the system and power flow control range with several FACTS devices is larger than that with only one such device. Therefore, the coordination of control performances of different devices is a very important issue for the future power system planning and operation.

CHAPTER 6

HARDWARE IMPLEMENTATION

6.1 INTRODUCTION TO HARDWARE IMPLEMENTATION

The basic power circuit scheme of a thyristor tap changer is shown this arrangement can give continuous voltage magnitude control by initiating the one set of thyristor valve conduction. A resistive load is connected to the output terminals of the thyristor tap changer. This load of course could be the line current in phase with the terminal voltage. The two voltages obtainable at the upper and lower taps, V_2 and V_1 respectively. The gating of the the thyristor valve is controlled by the delay angle α with respect to the voltage zero crossing of these voltage

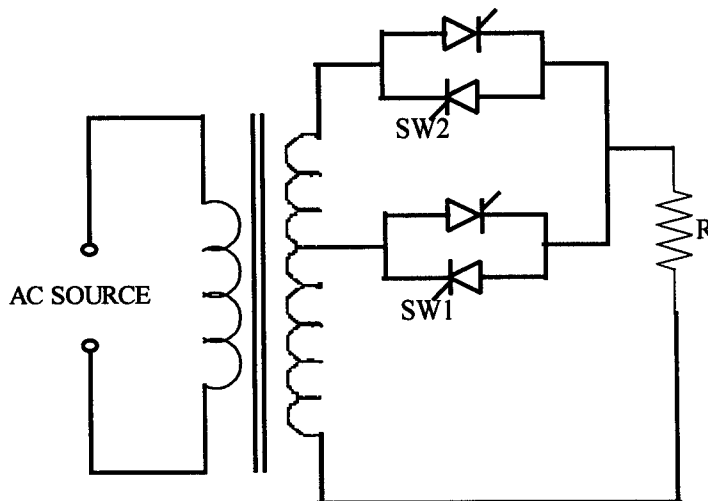


Figure 6.1.Basic thyristor tap changer circuit configuration

6.2 CIRCUIT DIAGRAM

The prototype circuit for TCPAR is shown and hardware is implemented for the same

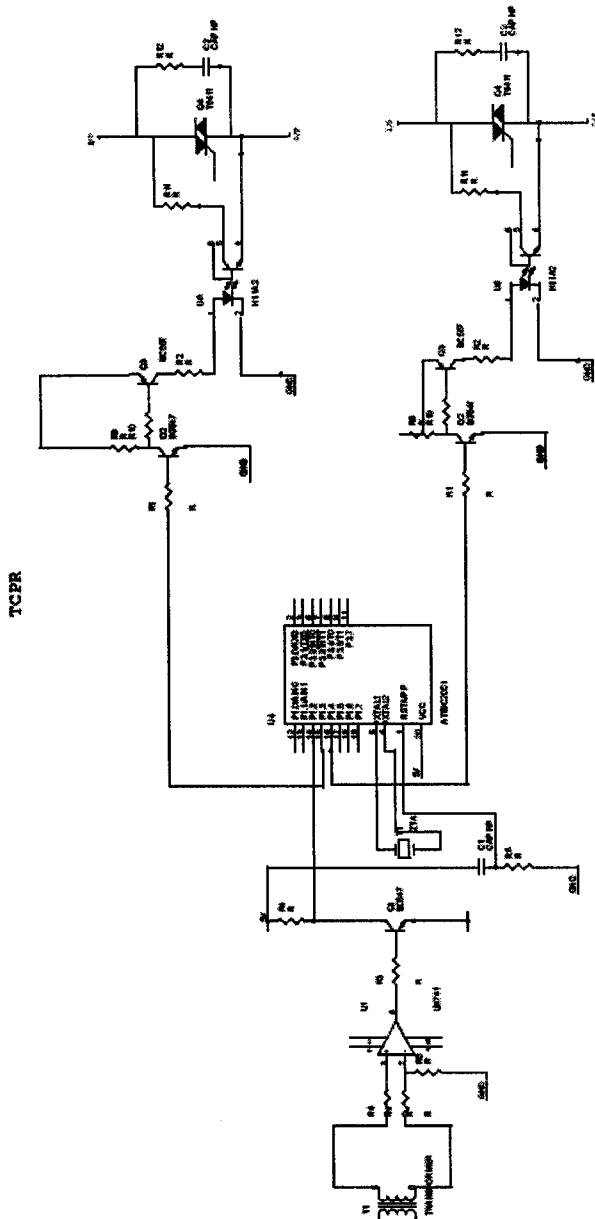


Figure 6.2.Circuit Diagram

6.3 CIRCUIT DISCRIPTION

6.3.1 Aim of this implementation

This arrangement gives continuous voltage magnitude control. This circuit concept that can handle voltage reversal can provide phase shift in either direction. This controller is TCPAR.

6.3.2 TCPAR prototype Circuit and Hardware Design

The prototype circuitry consists of the following hardware components and divisions. Design steps, circuit descriptions, and circuit drawings will be presented for each of the divisions.

The hardware design includes the following components viz..

1. Power Supply Unit
2. LM741 Comparator
3. ATMEL 89C2051
4. MOC3052-M opt isolators TRIAC drivers
5. Reset Inverter
6. OUTPUT unit.

The detailed descriptions about the above each component is presented well as below.

6.3.3 Power Supply Unit

The power supply unit provides the necessary power supply for the whole circuit. It gives a regulated power supply of +5V and $\pm 12V$ for running the processor and driving the relay. There is a step down transformer which is a two tapped one of which one

provides $230/9 - 0$ V and the other tapping provides $230/ 15 - 0 - 15$ V. The $9 - 0$ V provides the power supply for the micro controller and the other $15 - 0 - 15$ V provides power supply for the 7th and 4th Pin of the OP-AMP LM741. The power supply unit consists of the following IC's viz... 7805, 7812 and 7912 for voltage regulation

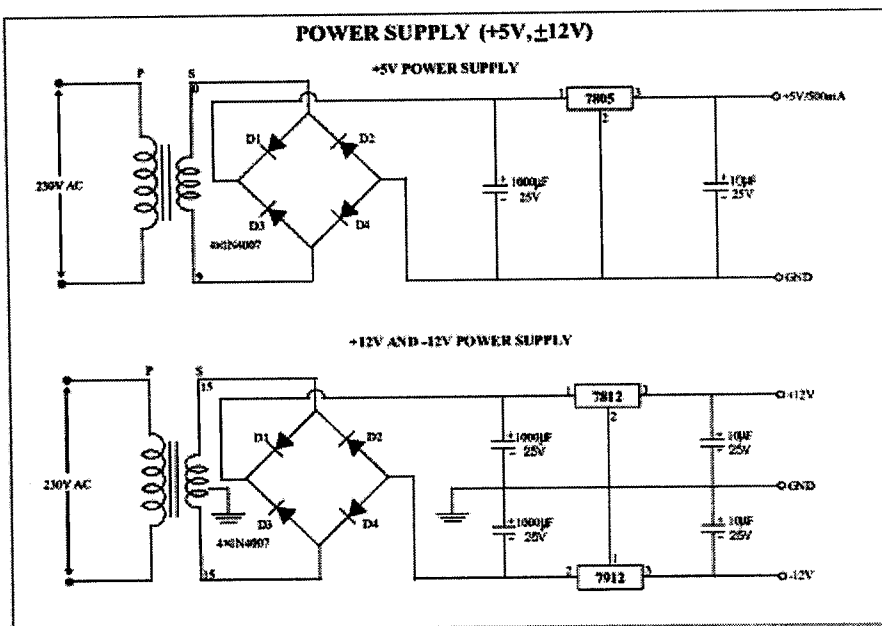


Figure 6.3. Power supply unit

6.3.4 LM 741 comparator

The LM741 series are general purpose operational amplifiers which feature improved performance over industry standards like the LM709. They are direct, plug-in replacements for the 709C, LM201, MC1439 and 748 in most applications. The amplifiers offer many features which make their application nearly foolproof: overload protection on the input and output, no latch-up when the common mode range is exceeded, as well as freedom from oscillations.

An op-amp comparator compares the reference ramp waveform at inverting input with a variable D input voltage at the non-inverting input and generates rectangular pulses at the output.

An op-amp comparator compares the reference ramp waveform at inverting input with a variable D input voltage at the non-inverting input and generates rectangular pulses at the output.

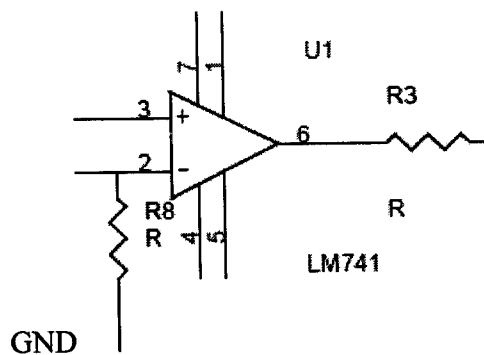


Figure 6.4. Comparator

6.3.5 Reset inverter

The reset inverter used here is 74LS14. Whenever the microcontroller is switched on it should be reset with the above said inverter and this is done only when the pulse comes from low to high. And this reset operation is done in order to avoid some unwanted operation and for proper functioning of the microcontroller

6.3.6 ATMEL 89C2051

The AT89C51 is a low-power, high performance 8-bit CMOS microcomputer with 4k Bytes of flash programmable and erasable read only memory (PEROM). The device is manufactured ATMEL's high density non volatile memory technology and is compatible with the industry standard MCS-51TM instruction set and pinout. The on-chip flash memory allows the programmable memory to be reprogrammed in-system or by a conventional non volatile memory programmer.

6.3.7 Pin description

Supply voltage of about 5v is given to VCC. Input from the comparator is given to the port p1.2 of AT89C2061. XTAL1 and XTAL2 are the input from the clock generator. The output is taken from the pin p1.3 and p1.4 to the MOC3052-M opt isolators TRIAC drivers.

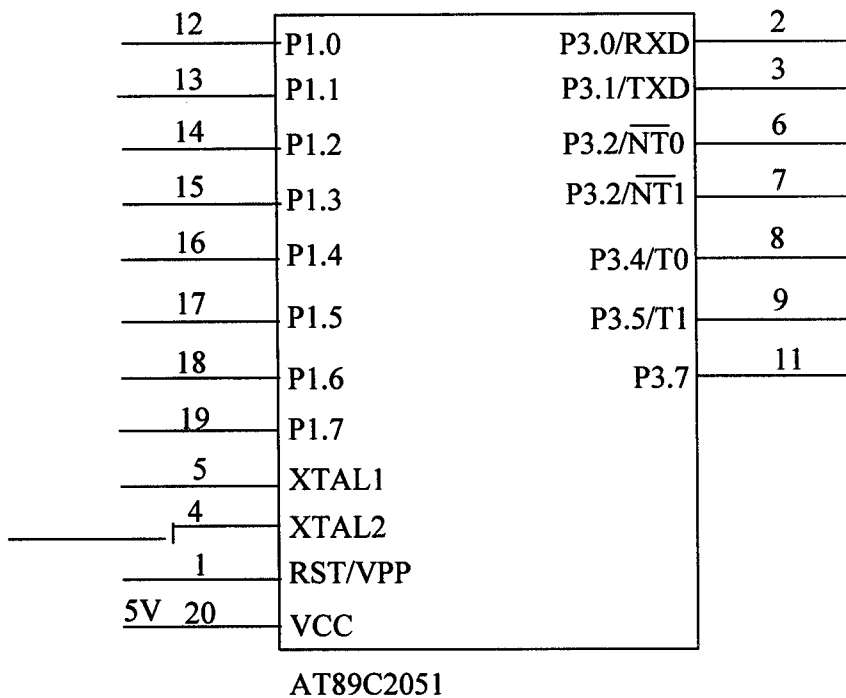


Figure 6.5. Pin diagram

Codings are generated using C language and compiled using MPLAB and the generated codings are shown in appendix

6.3.8 MOC3052-M OPTOISOLATORS TRIAC drivers

Description

The MOC3051-M and MOC3052-M consist of a AlGaAs infrared emitting diode optically coupled to a non-zero-crossing silicon bilateral AC switch (triac). These devices isolate low voltage logic from 115 and 240 Vac lines to provide random phase control of high current triacs or thyristors. These devices feature greatly enhanced static dv/dt capability to ensure stable switching performance of inductive loads.

Features

- Stability—IR emitting diode has low degradation
- High isolation voltage—minimum 7500 peak VAC
- Underwriters Laboratory (UL) recognized—File #E90700
- 600V peak blocking voltage
- VDE recognized (File #94766)
 - Ordering option V (e.g. MOC3052V-M)

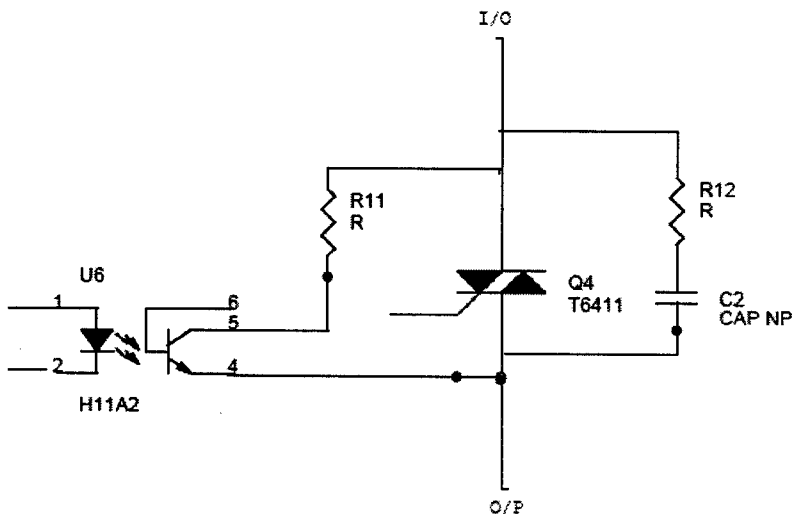


Figure 6.6. Optoisolator and TRIAC drivers

The output from AT89C2061 is given to these TRIAC drivers. There are two such drivers that drives two TRIACS. So that when the current crosses zero the previously conducting TRIAC turns off, then the TRIAC continues conduction until the next current zero is reached.

6.3.9 Output unit

The output of this circuit is seen from CRO from which the output voltage is controlled by varying the delay angle. This can provide voltage reversal which provides phase shift in either direction. Inspection of this output waveform indicates that by delaying the turn off valves from 0 to π , and output voltage between V_2 and V_1 can be obtained. The output wave form is shown below.

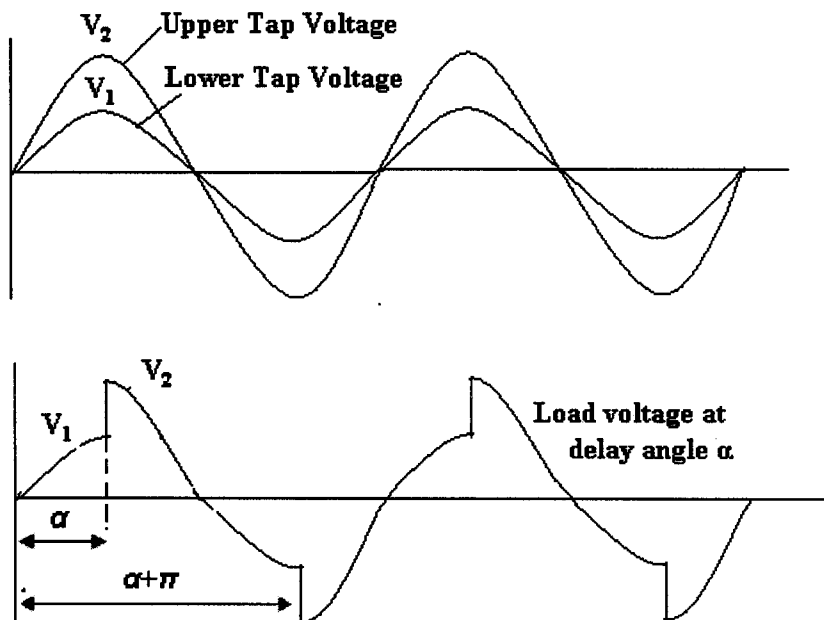


Figure 6.7. Output waveform

In this waveform by delaying the turn on of 6thr TRIAC valves from 0 to π and when the current crosses zero the conduction of the TRIAC is made for every zero crossings. An output voltage between V_2 and V_1 can be obtained.

CHAPTER7

CONCLUSION

The power flow can be rapidly and flexibly controlled by FACTS devices. In this paper, based on the steady state models of such devices, power flow controllability with single FACTS device is analytically investigated. When there are several such devices in the system, coordination of power flow control performances of these devices can be defined as an optimization problem. To solve this problem, an improved genetic algorithm based method has been developed. With this method, the power flow control ranges on one or a set of transmission lines in the power system installed with FACTS devices can be precisely computed. Examples demonstrate the power flow control range is dependent not only on the type of such device, but also on the initial power flow on the transmission line, and the coordinated control of several FACTS devices is more efficient than that of the single one.

APPENDIX 1- UPFC codings

```
% upfc based power flow solution using gernetic algorithm

clc;
clear all;
close all;

fprintf('Loading data from data file \n');

%run the data file
data;

fprintf('UPFC characteristics \n');

%upfc charactertics

%resistance
R=600;

%reactance
X=0.0143e4;

%real power
Pu=100*1e6;
%voltage rate

V=230;

%frequency
F=60;

%phase
teta=-pi:pi/6:pi;

%reference phae
tetal=pi/2;

%find the value a,b
for i=1:size(teta,2);
a(i)=((R*cos(teta(i)))+(X*sin(teta(i))))/(R^2+X^2);
b(i)=((R*cos(teta(i)))-(X*sin(teta(i))))/(R^2+X^2);
end
```

```

%referecne the node voltage
upq=235;
u=230;

for i=1:size(teta,2);
s(i)=upq*u*(a(i)+b(i)*j)*exp(tetal*j);
end

%find the real imaginary
reals=real(s/100);
imags=imag(s/100);

figure,plot(reals,imags);
title('real Vs imag');
xlabel('real values');
ylabel('imaginary values');

%14-bus data from data file

% Power flow solution
fprintf('power flow solution started \n');
ns=0;
ng=0;
Vm=0;
delta=0;
yload=0;
deltad=0;
nbus = length(busdata(:,1));
kb=[];
Vm=[];
delta=[];
Pd=[];
Qd=[];
Pg=[];
Qg=[];
Qmin=[];
Qmax=[];
Pk=[];
P=[];
Qk=[];
Q=[];
S=[];
V=[];

%upfcdata
upfcdata=Upfc.con;

```

```

for k=1:nbus
n=busdata(k,1);
kb(n)=busdata(k,2);
Vm(n)=busdata(k,3);
delta(n)=busdata(k,4);
Pd(n)=busdata(k,5);
Qd(n)=busdata(k,6);
Pg(n)=busdata(k,7);
Qg(n)=busdata(k,8);
Qmin(n)=busdata(k,9);
Qmax(n)=busdata(k,10);
Qsh(n)=busdata(k,11);
%find the valtage and power at node

if Vm(n) <= 0 Vm(n) = 1.0; V(n) = 1 + j*0;
else delta(n) = pi/180*delta(n);
if(i==upfcdata(1)|i==upfcdata(2))
V(n) = Vm(n)*(cos(delta(n)) + j*sin(delta(n)))+V;
P(n)=(Pg(n)-Pd(n)+Pu)/basemva;
Q(n)=(Qg(n)-Qd(n)+ Qsh(n))/basemva;
S(n) = P(n) + j*Q(n);
else
V(n) = Vm(n)*(cos(delta(n)) + j*sin(delta(n)));
P(n)=(Pg(n)-Pd(n))/basemva;
Q(n)=(Qg(n)-Qd(n)+ Qsh(n))/basemva;
S(n) = P(n) + j*Q(n);
end
end
end

```

```
fprintf('genetic algorithm implementation \n');
```

```
%genetic algorithm implementation
```

```

for i=1:n
%genetic algorithm optization
[X1 X2]=factsg(P(i),V(i));
%power
Pn(i)=X1(1);
%voltage
Vn(i)=X1(2);
%current
In(i)=X1(3);
%maximum
Mx(i)=X2;

```

```

end

%optimize value
Maxvalue=Mx(upfcdata(1));
Volt=Vn(upfcdata(1));

%phase
teta=-pi:pi/30:pi;

%reference phae

tetal=atan(Q(upfcdata(1))/P(upfcdata(1)));
mag=sqrt(Q(upfcdata(1))^2+P(upfcdata(1))^2)*1e3;

%find the value a,b
for i=1:size(teta,2);
a(i)=((R*cos(teta(i)))+(X*sin(teta(i))))/(R^2+X^2);
b(i)=((R*cos(teta(i)))-(X*sin(teta(i))))/(R^2+X^2);
end

%referecne the node voltage
upq=Volt;
u=Volt;

for i=1:size(teta,2);
sm(i)=upq*u*(a(i)+b(i)*j)*exp(tetal*j);
end

%find the real imagnary
reals=real(sm);
imags=imag(sm);

figure,plot(reals,imags);
title('real Vs imag after power flow solution ');
xlabel('real values ');
ylabel('imaginary values');

%conver the radians to degree
ph=tetal*180/pi;

fprintf('power and phase angle of system \n');
fprintf('power in mega watts %5.2f \n', mag);
fprintf('phase angle in pu %5.2f \n',ph);

```

APPENDIX 2-TCSC codings

```
%Tcsc characteristics
%resistance
clc;
clear all;
close all;

fprintf('Loading data from data file \n');

%run the data file
data1;

R=600;

%reactance
X=0.0143e4;

%real power
Pu=100*1e6;
%voltage rate
V=230;

%frequency
F=60;

%phase
teta=-pi:pi/48:pi;

%reference phae
tetal=pi/2;

%find the value a,b
for i=1:size(teta,2);
a(i)=((R*cos(teta(i)))+(X*sin(teta(i))))/(R^2+X^2);
b(i)=((R*cos(teta(i)))-(X*sin(teta(i))))/(R^2+X^2);
end

%referecne the node voltage
upq=235;
u=230;

for i=1:size(teta,2);
s(i)=upq*u*(a(i)+b(i)*j)^2*exp(tetal*j);
```

```

end

%find the real imaginary
realsa=real(s/100);
imagsa=imag(s/100);

% Power flow solution
fprintf('power flow solution started \n');
ns=0;
ng=0;
Vm=0;
delta=0;
yload=0;
deltad=0;
nbus = length(busdata(:,1));
kb=[];
Vm=[];
delta=[];
Pd=[];
Qd=[];
Pg=[];
Qg=[];
Qmin=[];
Qmax=[];
Pk=[];
P=[];
Qk=[];
Q=[];
S=[];
V=[];

%Tcscdata
Tcscdata=Tcsc.con;

for k=1:nbus
n=busdata(k,1);
kb(n)=busdata(k,2);
Vm(n)=busdata(k,3);
delta(n)=busdata(k,4);
Pd(n)=busdata(k,5);
Qd(n)=busdata(k,6);
Pg(n)=busdata(k,7);
Qg(n)=busdata(k,8);
Qmin(n)=busdata(k,9);

```

```

Qmax(n)=busdata(k, 10);
Qsh(n)=busdata(k, 11);
%find the valtage and power at node

if Vm(n) <= 0  Vm(n) = 1.0; V(n) = 1 + j*0;
  else delta(n) = pi/180*delta(n);
    if(i==Tcscdata(1)|i==Tcscdata(2))
      V(n) = Vm(n)*(cos(delta(n)) + j*sin(delta(n)))+V;
      P(n)=(Pg(n)-Pd(n)+Pu)/basemva;
      Q(n)=(Qg(n)-Qd(n)+ Qsh(n))/basemva;
      S(n) = P(n) + j*Q(n);
    else
      V(n) = Vm(n)*(cos(delta(n)) + j*sin(delta(n)));
      P(n)=(Pg(n)-Pd(n))/basemva;
      Q(n)=(Qg(n)-Qd(n)+ Qsh(n))/basemva;
      S(n) = P(n) + j*Q(n);
    end
  end
end
end

```

```

fprintf('genetic algorithm implementation \n');

```

```

%genetic algorithm implementation

```

```

for i=1:n
  %genetic algorithm optization
  [X1 X2]=factsg(P(i),V(i));
  %power
  Pn(i)=X1(1);
  %voltage
  Vn(i)=X1(2);
  %current
  In(i)=X1(3);
  %maximum
  Mx(i)=X2;
end

```

```

%optimize value
Maxvalue=Mx(Tcscdata(1));
Volt=Vn(Tcscdata(1));

```

```

%phase
teta=-pi:pi/30:pi;

```

```

%reference phae

tetal=atan(Q(Tcscdata(1))/P(Tcscdata(1)));
mag=sqrt(Q(Tcscdata(1))^2+P(Tcscdata(1))^2)*1e3;

%find the value a,b
for i=1:size(teta,2);
a(i)=((R*cos(teta(i)))+(X*sin(teta(i))))/(R^2+X^2);
b(i)=((R*cos(teta(i)))-(X*sin(teta(i))))/(R^2+X^2);
end

%referecne the node voltage
upq=Volt;
u=Volt;

for i=1:size(teta,2);
    sm(i)=upq*u*(a(i)+b(i)*j)^2*exp(tetal*j);
end

%find the real imaginary
reals=real(sm);
imags=imag(sm);

figure,plot(reals,imags);
title('real Vs imag');
xlabel('real values');
ylabel('imaginary values');

figure,plot(realsa,imagsa);
title('real Vs imag after power flow solution ');
xlabel('real values ');
ylabel('imaginary values');

%conver the radians to degree
ph=tetal*180/pi;

fprintf('power and phase angle of system \n');
fprintf('power in mega watts %5.2f \n', mag);
fprintf('phase angle in pu %5.2f \n',ph);

```

APPENDIX 3-TCPAR codings

```
%Tcpr charactertics
%resistance
clear all;
R=600;
data2;
%reactance
X=0.0143e4;

%real power
Pu=100*1e6;
%voltage rate
V=230;

%frequency
F=60;

%phase
teta=pi/3:pi/48:pi/2;

%reference phae
tetal=-pi/2;

%find the value a,b
for i=1:size(teta,2);
a(i)=((R*cos(teta(i)))+(X*sin(teta(i))))/(R^2+X^2);
b(i)=((R*cos(teta(i)))-(X*sin(teta(i))))/(R^2+X^2);
end

%referecne the node voltage
upq=235;
u=230;

for i=1:size(teta,2);
s(i)=upq*u*(a(i)+b(i)*j)*exp(tetal*j);
end

%find the real imagnary
reals=real(s/100);
imags=imag(s/100);

figure,plot(reals,imags);
title('real Vs imag');
xlabel('real values');
```

```
ylabel('imaginary values');
```

```
% Power flow solution
```

```
fprintf('power flow solution started \n');
```

```
ns=0;
```

```
ng=0;
```

```
Vm=0;
```

```
delta=0;
```

```
yload=0;
```

```
deltad=0;
```

```
nbus = length(busdata(:,1));
```

```
kb=[];
```

```
Vm=[];
```

```
delta=[];
```

```
Pd=[];
```

```
Qd=[];
```

```
Pg=[];
```

```
Qg=[];
```

```
Qmin=[];
```

```
Qmax=[];
```

```
Pk=[];
```

```
P=[];
```

```
Qk=[];
```

```
Q=[];
```

```
S=[];
```

```
V=[];
```

```
%Tcprdata
```

```
Tcprdata=Tcpr.con;
```

```
for k=1:nbus
```

```
n=busdata(k,1);
```

```
kb(n)=busdata(k,2);
```

```
Vm(n)=busdata(k,3);
```

```
delta(n)=busdata(k,4);
```

```
Pd(n)=busdata(k,5);
```

```
Qd(n)=busdata(k,6);
```

```
Pg(n)=busdata(k,7);
```

```
Qg(n)=busdata(k,8);
```

```
Qmin(n)=busdata(k,9);
```

```
Qmax(n)=busdata(k,10);
```

```
Qsh(n)=busdata(k,11);
```

```
%find the valtage and power at node
```

```
if Vm(n) <= 0 Vm(n) = 1.0; V(n) = 1 + j*0;
```

```

else delta(n) = pi/180*delta(n);
    if(i==Tcprdata(1)|i==Tcprdata(2))
    V(n) = Vm(n)*(cos(delta(n)) + j*sin(delta(n)))+V;
    P(n)=(Pg(n)-Pd(n)+Pu)/basemva;
    Q(n)=(Qg(n)-Qd(n)+ Qsh(n))/basemva;
    S(n) = P(n) + j*Q(n);
    else
        V(n) = Vm(n)*(cos(delta(n)) + j*sin(delta(n)));
        P(n)=(Pg(n)-Pd(n))/basemva;
        Q(n)=(Qg(n)-Qd(n)+ Qsh(n))/basemva;
        S(n) = P(n) + j*Q(n);
    end
end
end
end

```

```
fprintf('genetic algorithm implementation \n');
```

```
%genetic algorithm implementation
```

```

for i=1:n
    %genetic algorithm optization
    [X1 X2]=factsg(P(i),V(i));
    %power
    Pn(i)=X1(1);
    %voltage
    Vn(i)=X1(2);
    %current
    In(i)=X1(3);
    %maximum
    Mx(i)=X2;
end

```

```

%optimize value
Maxvalue=Mx(Tcprdata(1));
Volt=Vn(Tcprdata(1));

```

```

%phase
teta=pi/3:pi/48:pi/2;

```

```
%reference phae
```

```

tetal=atan(Q(Tcprdata(1))/P(Tcprdata(1)));
mag=sqrt(Q(Tcprdata(1))^2+P(Tcprdata(1))^2)*1e3;

```

```

%find the value a,b
for i=1:size(teta,2);
a(i)=((R*cos(teta(i)))+(X*sin(teta(i))))/(R^2+X^2);
b(i)=((R*cos(teta(i)))-(X*sin(teta(i))))/(R^2+X^2);
end

```

```

%referecne the node voltage
upq=Volt;
u=Volt;

```

```

for i=1:size(teta,2);
    sm(i)=upq*u*(a(i)+b(i)*j)*exp(tetal*j);
end

```

```

%find the real imaginary
reals=real(sm);
imags=imag(sm);

```

```

figure,plot(reals,imags);
title('real Vs imag after power flow solution ');
xlabel('real values ');
ylabel('imaginary values');

```

```

%conver the radians to degree
ph=tetal*180/pi;

```

```

fprintf('power and phase angle of system \n');
fprintf('power in mega watts %5.2f \n', mag);
fprintf('phase angle in pu %5.2f \n',ph);

```

APPENDIX 4-Genetic Algorithm implementation

```
function
opt_param=geneticm(popsiz, objfunc, N, minmax, nbit,
pc, pm, maxg)
%Initialize generation counter, 'gc', and
stopping flag 'stop'.
nbit
gc=1;
stop=0;
%select random initial decimal values of
parameters in the
%popsize x N matrix (refer Note1)
for i=1:popsize
for j=1:N
inivar(i,j)=round(rand*(2^nbit(j)-1));
end;
end;
%Convert decimal values to binary bits and
generate
%popsize x lchrom
%bitmatrix where lchrom is the length of a
chromosome (refer note
%2)
lchrom=sum(nbit);
bitmat=zeros(popsize, lchrom);
for I=1: popsize
k=lchrom;
for j=N:-1:1
x=inivar(I,j);
for m=1:nbit(j)
bitmat(I,k)=rem(x,2);
x=fix(x/2);
k=k-1;
end;
end;
end;
%MAIN LOOP STARTS HERE
while(stop==0)
gc
%Calculate actual parameter values from bitmatrix
(refer
%note 3)
for j=1:N
for i=1:popsize
```

```

param(i,j)=minmax(j,1)...
    +(minmax(j,2)-minmax(j,1))/...
    (2^nbit(j)-1)*inivar(i,j);
end;
end;
%Calculate fitness values
sumfit=0;
for i=1:popsiz
    argu=param(i,1:N);
    fitness(i)=feval(objfunc,argu);
    sumfit=sumfit+fitness(i);
end
avgfit=sumfit/popsiz;
%parameters giving max fitness are given out as
%optimum parameters
[maxfit,index]=max(fitness);
opt_param=param(index,:);
fit_ratio=avgfit/maxfit;
%Build an array of avg&max fitness values and
%record them generation-wise
af(gc)=avgfit;
mf(gc)=maxfit;
%generate mating pool through Roulette wheel
selection
sum=0;
for i=1:popsiz
    %Compute probability of selection of the ith
    chromosome
    ps=fitness(i)/sumfit;
    %Obtain cumulative sum of the selection
    probabilities
    sum=sum+ps;
    csum(i)=sum;
    end
    %randperm returns random sequencing of numbers
    from 1 to
    %popsiz.
    mplocation=randperm(popsiz);
    %The randomly spum RW selects jth
    chromosome&places it at
    %a
    %random location in mating pool. (refer Note 4)
    for i=1:popsiz
        rwspin=rand;
        for j=1:popsiz
            if(rwspin<=csum(j))
                for k=1:lchrom

```

```

mpool(mplocation(i),k)=bitmat(j,k);
end;
break;
else;
end;
end;
end;
end;
%Crossover operator
%Number of crossovers nc
nc=round(pc*popsize/2);
%Increment by 2 since crossover is pairwise
(refer note 5)
for i=1:2:nc
xsite=round(rand*lchrom);
for j=1:xsite
temp=mpool(i,j);
mpool((i+1),j)=temp;
end;
end;
%Mutation Operator
%Number
nm=round((pm*lchrom*popsize));
while(nm>0)
for i=1:nm
msite=round(rand*lchrom*popsize);
%msite is being worked out not just within a
%particular
%chromosome, but over the entire bitmatrix
if(msite==0)
msite=1;
% Since nm>0, make the 0 msite as 1 so that
% atleast
% One mutation does take place.
end;
% Location of the bit to be mutated
colm=rem(msite,lchrom);
if(colm==0)
colm=lchrom;
row=fix(msite/lchrom);
else
row=fix(msite/lchrom)+1;
end;
if(mpool(row,colm)==0)
mpool(row,colm)=1;
else
mpool(row,colm)=0;
end;
end;

```

```

end;
nm=0;
end;
% Decoding
% Identify the bits in a string corresponding to
a
% Parameter (refer note6)
for I=1:popsize
b1=0;
bn=0;
for j=1:N
sum=0;
n=nbit(j);
if(j==1)
b1=1;
else
b1=b1+nbit(j-1);
end;
bn=bn+nbit(j);
%Calculate the decimal value
for k=b1:bn
n=n-1
sum=sum+(mpool(I,k))*(2^n);
end;
var(I,j)=sum;
end;
end;
%Increment the generation counter
gc=gc+1
inivar=var;
bitmat=mpool;
%stopping criteria
if((gc>maxg)|(fit_ratio)>0.9999)
    stop=1;
else
    stop=0;
end;
end;
%MAIN LOOP ENDS
if(gc>maxg)
disp('GOAL NOT REACHED');
end;
kf=1:gc-1;
figure(2)
plot(kf,mf,'b',kf,af,'r')
legend('maxfit','avgfit')

```

```

function [y]=objfunc(x)
P=x(1);
V=x(2);
I=P/V;
sum=0;
for i = 1:14
    sum=sum+P;
end
sump=sum;
sum=0;
for i = 1:14
    sum=sum+(V-10e3);
end
sumV=sum;
sum=0;
for i = 1:14
    sum=sum+(I-30);
end
sumI=sum;
y = max(sump-5*sumV-5*sumI);

```

```

function[J] = objprocess(x)
%def gain const
GP=x(1);GQ=x(2);GV=x(3);
J=atan(GQ/GP);

```

APPENDIX 5-UPFC Datas

Bus No.	Mag p.u	Genertion		Load							
		MW	MVAr	MW	MVAr						
busdata =[1	1	1.06	0	0	0	0	0	0	0	0	0
	2	1	0	21.2	12.2	40	0	40	50	0	
	3	1	0	94.2	19.0	0	0	0	40	0	
	4	1	0	47.8	3.9	0	0	0	0	0	
	5	1	0	7.6	1.6	0	0	0	0	0	
	6	1	0	11.2	7.5	0	0	-6	24	0	
	7	1	0	0	0	0	0	0	0	0	
	8	1	0	0	0	0	0	-6	24	0	
	9	1	0	29.5	16.6	0	0	0	0	0	
	10	1	0	9.0	5.8	0	0	0	0	0	
	11	1	0	3.5	1.8	0	0	0	0	0	
	12	1	0	6.1	1.6	0	0	0	0	0	
	13	1	0	13.5	5.8	0	0	0	0	0	
	14	1	0	14.9	5.6	0	0	0	0	0	0];

linedata =[1	2	0.01938	0.05917	0.0264	1
	1	0.05403	0.22304	0.0246	1
	2	0.04699	0.19797	0.0219	1
	2	0.05811	0.17632	0.0187	1
	2	0.05695	0.17388	0.0170	1
	3	0.06701	0.17103	0.0173	1
	4	0.01335	0.04211	0.0064	1
	4	0	0.20912	0	1
	4	0	0.55618	0	1
	5	0	0.25202	0	1
	6	0.09498	0.19890	0	1
	6	0.12291	0.25581	0	1
	6	0.06615	0.13027	0	1
	7	0	0.17615	0	1
	7	0	0.11001	0	1
	9	0.03181	0.08450	0	1
	9	0.12711	0.27038	0	1
	10	0.08205	0.19207	0	1
	12	0.22092	0.19988	0	1
	13	0.17093	0.34802	0	1];

Upfc.con = [3	4	100	69	60	60	0.0143
0.0001	0.105	1	0.001	1	0.001	1.05
1.02	100	200	100	200	0.0001	0.101
0.002	0.095	100	200	0.8	0.2	1.2

0.8];
basemva=1000;
accuracy=0.001;
maxiter=100;

APPENDIX 6-TCSC Datas

```

          Genertion   Load
Bus No. Mag
      p.u MW   MVAr MW   MVAr
busdata =[1  1  1.06  0  0  0  0  0  0  0  0
           2  2  1  0  21.2  12.2  40  0  40  50  0
           3  0  1  0  94.2  19.0  0  0  0  40  0
           4  0  1  0  47.8  3.9  0  0  0  0  0
           5  0  1  0  7.6  1.6  0  0  0  0  0
           6  0  1  0  11.2  7.5  0  0  -6  24  0
           7  0  1  0  0  0  0  0  0  0  0
           8  0  1  0  0  0  0  0  -6  24  0
           9  0  1  0  29.5  16.6  0  0  0  0  0
          10  0  1  0  9.0  5.8  0  0  0  0  0
          11  0  1  0  3.5  1.8  0  0  0  0  0
          12  0  1  0  6.1  1.6  0  0  0  0  0
          13  0  1  0  13.5  5.8  0  0  0  0  0
          14  0  1  0  14.9  5.6  0  0  0  0  0];

linedata =[1  2  0.01938  0.05917  0.0264  1
           1  5  0.05403  0.22304  0.0246  1
           2  3  0.04699  0.19797  0.0219  1
           2  4  0.05811  0.17632  0.0187  1
           2  5  0.05695  0.17388  0.0170  1
           3  4  0.06701  0.17103  0.0173  1
           4  5  0.01335  0.04211  0.0064  1
           4  7  0  0.20912  0  1
           4  9  0  0.55618  0  1
           5  6  0  0.25202  0  1
           6  11  0.09498  0.19890  0  1
           6  12  0.12291  0.25581  0  1
           6  13  0.06615  0.13027  0  1
           7  8  0  0.17615  0  1
           7  9  0  0.11001  0  1
           9  10  0.03181  0.08450  0  1
           9  14  0.12711  0.27038  0  1
          10  11  0.08205  0.19207  0  1
          12  13  0.22092  0.19988  0  1
          13  14  0.17093  0.34802  0  1 ];

Tcsc.con = [3  4  100  69  60  60  0.0143
            0.0001  0.105  1  0.001  1  0.001  1.05
            1.02  100  200  100  200  0.0001  0.101
            0.002  0.095  100  200  0.8  0.2  1.2
            0.8 ];

basemva=1000;
accuracy=0.001;
maxiter=100;

```

APPENDIX 7-TCPAR Datas

```

          Genertion   Load
Bus No. Mag
      p.u MW      MVar MW      MVar
busdata =[1  1  1.06  0  0  0  0  0  0  0  0
           2  2  1  0  21.2  12.2  40  0  40  50  0
           3  0  1  0  94.2  19.0  0  0  0  40  0
           4  0  1  0  47.8  3.9  0  0  0  0  0
           5  0  1  0  7.6  1.6  0  0  0  0  0
           6  0  1  0  11.2  7.5  0  0  -6  24  0
           7  0  1  0  0  0  0  0  0  0  0
           8  0  1  0  0  0  0  0  -6  24  0
           9  0  1  0  29.5  16.6  0  0  0  0  0
          10  0  1  0  9.0  5.8  0  0  0  0  0
          11  0  1  0  3.5  1.8  0  0  0  0  0
          12  0  1  0  6.1  1.6  0  0  0  0  0
          13  0  1  0  13.5  5.8  0  0  0  0  0
          14  0  1  0  14.9  5.6  0  0  0  0  0];

linedata =[1  2  0.01938  0.05917  0.0264  1
            1  5  0.05403  0.22304  0.0246  1
            2  3  0.04699  0.19797  0.0219  1
            2  4  0.05811  0.17632  0.0187  1
            2  5  0.05695  0.17388  0.0170  1
            3  4  0.06701  0.17103  0.0173  1
            4  5  0.01335  0.04211  0.0064  1
            4  7  0  0.20912  0  1
            4  9  0  0.55618  0  1
            5  6  0  0.25202  0  1
            6  11  0.09498  0.19890  0  1
            6  12  0.12291  0.25581  0  1
            6  13  0.06615  0.13027  0  1
            7  8  0  0.17615  0  1
            7  9  0  0.11001  0  1
            9  10  0.03181  0.08450  0  1
            9  14  0.12711  0.27038  0  1
            10  11  0.08205  0.19207  0  1
            12  13  0.22092  0.19988  0  1
            13  14  0.17093  0.34802  0  1 ];

Tcpr.con = [3  4  100  69  60  60  0.0143
0.0001  0.105  1  0.001  1  0.001  1.05
1.02  100  200  100  200  0.0001  0.101
0.002  0.095  100  200  0.8  0.2  1.2
0.8 ];

basemva=1000;
accuracy=0.001;
maxiter=100;

```

APPENDIX 8-MICROCONTROLLER CODINGS

```
#include<reg51.h>
void delay(unsigned int);
sbit input    = P1^2;
sbit output1  = P1^3;
sbit output2  = P1^4;
sbit output3  = P1^5;
sbit output4  = P1^6;
main()
{
    output1=output2=0;
    while(1)
    {
        while(!input);
        output2=output4=0;
        delay(38);
        output1=output3=1;
        while(input);
        output1=output3=0;
        delay(38);
        output2=output4=1;
    }
}
void delay(unsigned int del)
{
    while(del--);
}
```

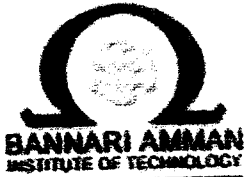
REFERENCES

- [1] G. N. Taranto and L. M. V. G. Pinto *et al.*, "Representation of FACTS devices in power system economic dispatch," *IEEE Trans.on PowerSystemss*, vol. 7, no. 2, pp. 572-576, 1992.
- [2] L. Gyogyi, "Unified power-flow control concept for flexible AC transmission systems," *IEE Proc.-C*, vol. 139, no. 4, pp. 323-331, 1992.
- [3] M. Noroakin and L. Aengquist *el al.*, "Use of UPFC Soar optimal power flow Control," in *Stockholm Power Tech Conference*, Stockholm, Sweden, June 1995, Paper SPT PS 16-05-0295, pp. 506-511.
- [4] IR. J. Nelsonand J. Bian *etul.*, "Transmission series power flaw control," *ERE Trans. on Power Delivery*. vol. 10, no. I, pp. 504-510, 1995.
- [5] Hingorani, N.G., "Flexible AC Transmission", *IEEE Spectrum*, April 1993, p. 40-44

NATIONAL CONFERENCE

ON

CUTTING EDGE TECHNOLOGIES IN POWER
CONVERSION AND INDUSTRIAL ENERGY
(PCID - 2005)



Strive Ahead

Department of Electrical & Electronics Engineering
Bannari Amman Institute of Technology
Sathyamangalam – 638 401, Tamilnadu



March 21 - 23 2005

Date: 21-02-2005

Organizing Committee

To
Ms. N.Geetha Rani
Final M.E. (P.E.&D)
Department of Electrical & Electronics Engg.
Kumaraguru College of Technology
Coimbatore

Chairman

Title of paper : POWER FLOW OPTIMIZATION WITH FACTS DEVICES IN
INTERCONNECTED POWER SYSTEMS

Sri S.V. Balasubramaniam
Managing Trustee, BIT

Dear Ms. N.Geetha Rani

Congratulations! Thank you for your interest in PCID 2005.
We acknowledge with thanks the receipt of your paper and your registration fees. Your paper has been accepted for oral presentation at PCID 2005. The list of accepted papers uploaded on the website www.bitsathy.ac.in is updated periodically.

Chairman

This is a pro-author Conference and your personal participation is absolutely essential. Kindly confirm your participation for PCID 2005 by return mail.

Dr. A. Shanmugam
Principal, BIT

We will provide free boarding and lodging for all the participants within our campus. To serve you better, we would request you to furnish the following details as soon as possible.

Chairman

Dr. G. Gurusamy
Dean/EEE, BIT

1. Name of the participant
2. Telephone number
3. Address
4. E-mail address

We are personally anxious to see you here at Sathyamangalam during the Conference. Please treat this letter as an official document for all conference related activities. The schedule for presentation will be informed at the time of registration. Your presentation would be for 15 minutes. You may present your paper with the help of OHP transparencies or with power point slides. Best paper in each session will be rewarded. Please feel free to write to us in case you have any query. Best wishes & Awaiting your active participation in PCID 2005

Chairman

Dr. A. Nirmal Kumar
HOD/EEE, BIT

Organizing Secretaries

Prof. R. Senthilkumar
Mr. R. Bharanikumar

Joint Secretary

Mr. J. Charles Arokiaraj
Mr. P.S. Mayurappriyan

Dr. A. Nirmal Kumar
Convener, PCID – 2005,
Bannari Amman Institute of Technology,
Sathyamangalam,
Tamilnadu

* - Details available in website

Bannari Amman Institute of Technology, Sathyamangalam – 638 401, Erode Dt, Tamilnadu
Tel: 04295 – 221289. Ext:522, Fax: (91 – 4295) 223775;
E – mail: pcid2005@rediffmail.com; Website: bitsathy.ac.in/PCID2005

**FIRST NATIONAL CONFERENCE ON
"CUTTING EDGE TECHNOLOGIES IN POWER CONVERSION AND INDUSTRIAL DRIVES"**

PCID-2005

Organised by : Department of Electrical & Electronics Engineering
(Accredited by NBA,AICTE New Delhi)

Sponsored by : Council of Scientific and Industrial Research(CSIR), New Delhi

THIS CERTIFIES THAT

Prof./Dr./Mr./Ms. N. GEETHA RANI

*has participated in the NATIONAL CONFERENCE on "POWER CONVERSION AND INDUSTRIAL DRIVES",
PCID-2005 held during 25 - 26 March 2005 and has presented a paper titled Power Flow Optimization
with FACTS Devices in Interconnected Power Systems.*

in the session PS-2 of the conference.

Dr. A. Nirmal Kumar
Convenor PCID-2005

Dr. G. Gurusamy
Session Chair
PCID-2005

Dr. A. Shanmugam

Dr. G. Gurusamy
Dean EEE

Dr. A. Shanmugam
Principal